Epithelial Malignant Tumors of the Cervix: Squamous Carcinoma

7

Michael P. Crawford, Taylor M. Jenkins, and Anne M. Mills

Contents

M. P. Crawford · T. M. Jenkins · A. M. Mills (✉)
Department of Pathology, University of Virginia,
Charlottesville, VA, USA
e-mail: MPC5U@hscmail.mcc.virginia.edu; TEM9SF@hscmail.mcc.virginia.edu; amm7r@virginia.edu

R. A. Soslow et al. (eds.), *Atlas of Diagnostic Pathology of the Cervix*, https://doi.org/10.1007/978-3-030-49954-9_7

7.1 Etiology

More than 95% of cervical squamous cell carcinomas are attributable to high-risk human papillomavirus (HPV) infection [1]. Occasional HPV-negative cases and cases associated with low-risk HPV do occur, but they comprise a small minority of the overall cervical squamous cancer disease burden [2, 3]. The high-risk HPV types 16 and 18 constitute the most clinically significant drivers, underlying 70% of all cervical squamous cancers; other contributors include the known carcinogenic types 31, 33, 35, 39, 45, 51, 52, 56, 58, and 59, as well as the likely carcinogenic types 26, 53, 66, 67, 68, 70, 73, and 82 [1, 4, 5].

Productive infection with high-risk subtypes leads to expression of the viral oncogenes E6 and E7 in dividing epithelial cells. This first manifests as a high-grade squamous intraepithelial lesion (HSIL), a non-obligate precursor to squamous cell carcinoma. The progression from HSIL to invasive carcinoma requires additional genetic and epigenetic alterations and may take several decades to fulminate. Somatic alterations including the PI3K/MAPK and TGFβ signaling pathways have been implicated, as have the genes *ERBB3*, *CASP8*, *HLA-A*, *SHKBP1*, and *TGFBR2* [6]. Contributing factors also include hypermethylation of CpG islands in tumor suppressor gene promotors, as well as patient variables such as immunosuppression and smoking [7, 8].

7.2 Clinical Features

Cervical squamous cell carcinoma is the fourth most common cancer in women worldwide [9]. The majority of cases occur in low- and middle-income countries, where screening and HPV vaccination programs are not routinely implemented [9], but women in economically developed countries remain at risk owing to incomplete penetrance of these preventative measures.

Symptoms may be entirely absent for early-stage tumors. More advanced cancers can present as abnormal vaginal bleeding, pelvic pain, and discharge, as well as symptoms related to ureteric obstruction, vesicovaginal fistulas, and/or rectovaginal fistulas.

7.3 Macroscopic Appearance

The gross appearance of cervical squamous cell carcinoma ranges from subtle to overt. Early invasion may manifest macroscopically as erythematous, erosive, or minimally raised areas on an otherwise unremarkable cervix. Advanced tumors may be either endophytic with surface mucosal irregularities and puckering, or exophytic with a polypoid or papillary appearance. The tumors are often friable and necrotic.

7.4 Microscopic Appearance

Cervical squamous cell carcinoma arises in association with HSIL and most often manifests as an infiltrative population of cells arranged in irregular nests, anastomosing cords, and solid sheets (Fig. 7.1). The constituent cells can be uniform and low-grade to wildly anaplastic, and mitotic figures are often abundant (Figs. 7.2 and 7.3). The background stroma typically shows prominent desmoplasia, sometimes with a marked lymphoid response. Necrosis is commonly encountered and is often located in the center of tumor cell nests (Fig. 7.4). Histologic subtypes include keratinizing, nonkeratinizing, papillary, basaloid, warty-type/condylomatous, and lymphoepithelioma-like tumors. Neither grade nor histologic subtype has a significant impact on prognosis.

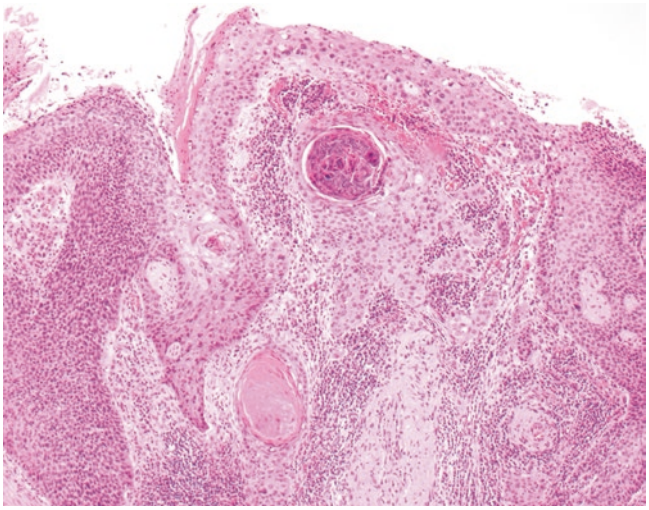

Fig. 7.1 Squamous cell carcinoma of the cervix: An infiltrative population of malignant cells originating in the squamous mucosa

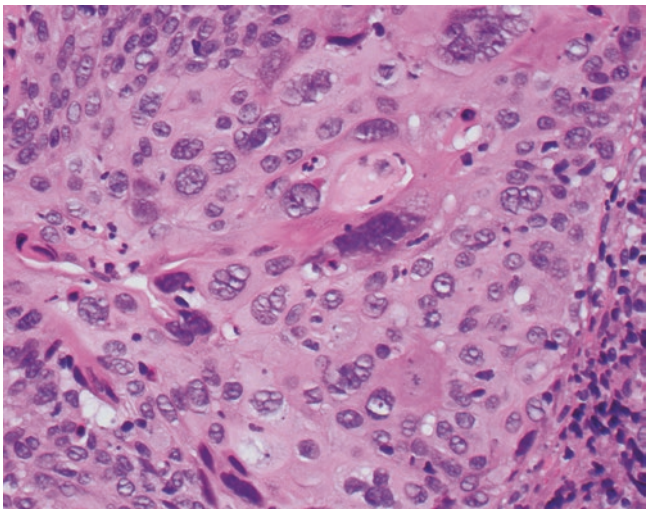

Fig. 7.3 Squamous cell carcinoma of the cervix: Marked anaplasia including cells with bizarre hyperchromatic nuclei

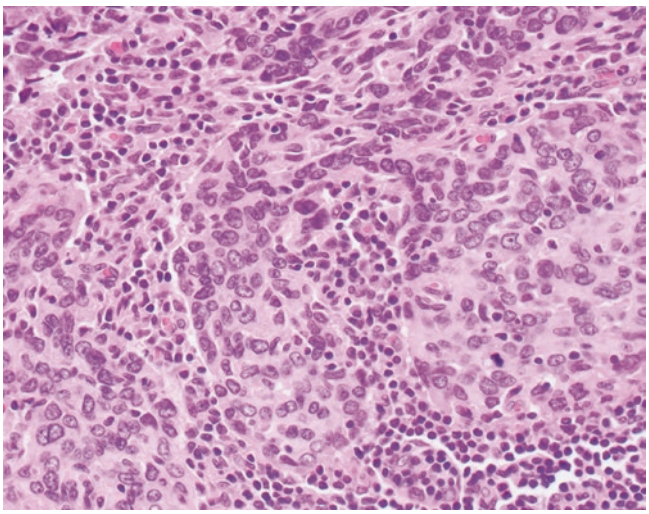

Fig. 7.2 Squamous cell carcinoma of the cervix: Atypical but relatively monotonous cells with moderate amounts of eosinophilic cytoplasm

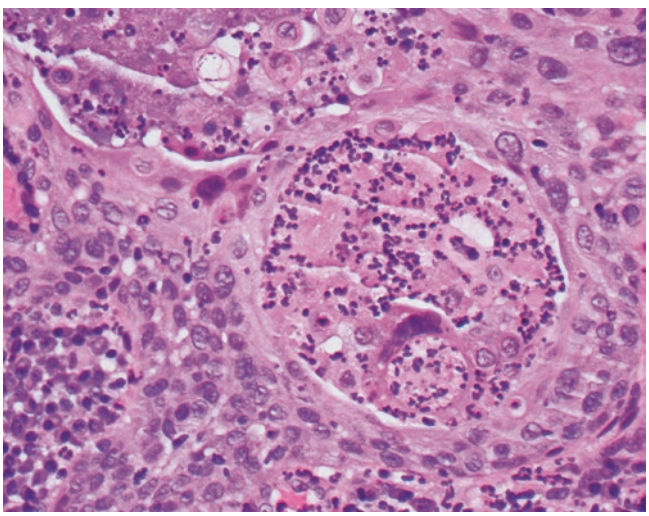

Fig. 7.4 Squamous cell carcinoma: Necrosis associated with a tumor nest

7.4.1 Histologic Subtypes

7.4.1.1 Keratinizing Squamous Cell Carcinoma

Keratinizing squamous cell carcinoma has a well-differentiated, mature appearance characterized by polygonal cells with moderate to abundant amounts of dense eosinophilic cytoplasm, keratohyalin granules, and intercellular bridges (Fig. 7.5). Tumor cell nuclei typically show coarse, clumped chromatin with variable pleomorphism, ranging from relatively uniform to markedly atypical. Mitotic figures, including abnormal mitoses, are common. Necrosis and keratinization are often seen at the center of tumor cell nests, and well-formed keratin pearls may be present (Fig. 7.6). Invasion often assumes a "saw-tooth" pattern with infiltrative nests, tongues, and cords. Budding invasion characterized by single cells and minute cell clusters can occur, as can complete replacement of the stroma by tumor. Occasionally, a foreign body giant cell reaction is present in association with extracellular keratin (Fig. 7.7).

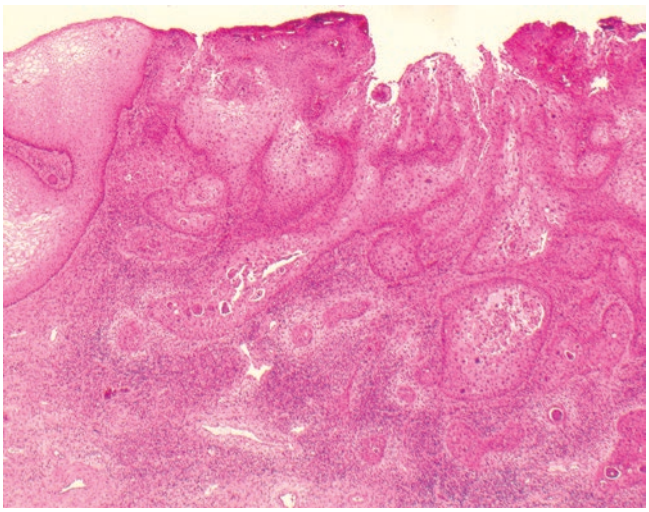

Fig. 7.5 Keratinizing squamous cell carcinoma: Mature-appearing cells with abundant eosinophilic cytoplasm invading as infiltrative nests and tongues

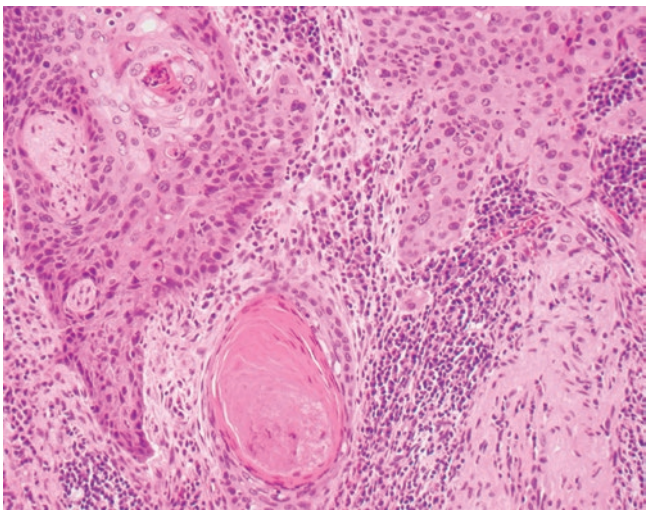

Fig. 7.6 Keratinizing squamous cell carcinoma: Jagged nest of invasion with associated keratin pearl and robust associated lymphoid response

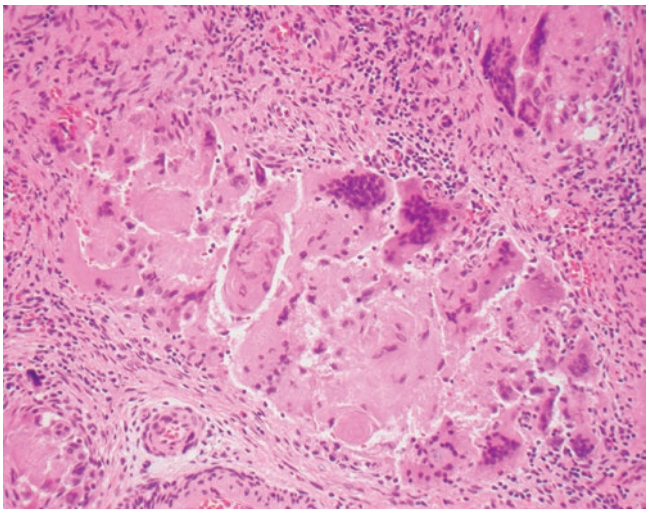

Fig. 7.7 Multinucleated giant cell reaction: Extracellular keratin in squamous cell carcinoma can be associated with a prominent giant cell response

7.4.1.2 Non-Keratinizing Squamous Cell Carcinoma

Non-keratinizing squamous cell carcinoma encompasses moderately to poorly differentiated tumors that may show keratinization, but lack the keratin pearls and keratohyalin granules characteristic of keratinizing squamous cell carcinomas (Figs. 7.8 and 7.9). Intercellular bridging can be present but is less common than in keratinizing tumors. Pleomorphism is often marked in these tumors.

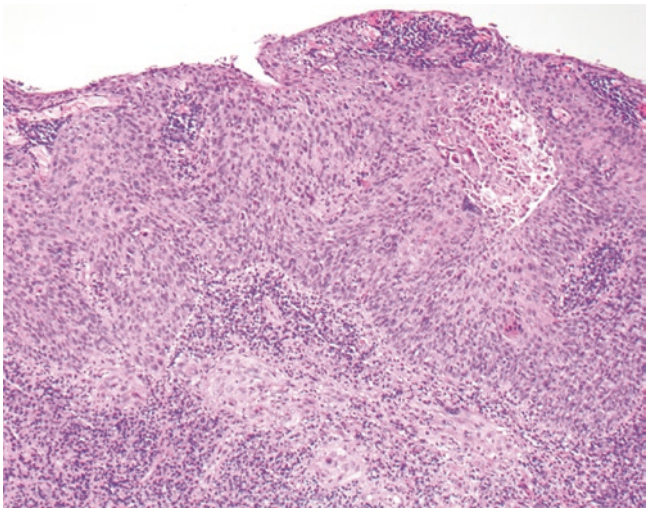

Fig. 7.8 Non-keratinizing squamous cell carcinoma: Malignant cells with scant cytoplasm and limited keratinization invading as jagged tongues

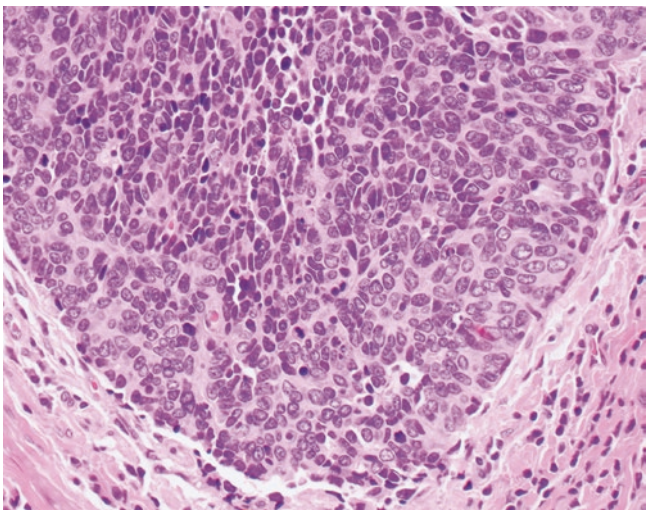

Fig. 7.9 Non-keratinizing poorly differentiated squamous cell carcinoma: Malignant cells with high nuclear:cytoplasmic ratios and no appreciable keratin

7.4.1.3 Basaloid Squamous Cell Carcinoma

Basaloid squamous cell carcinomas are immature-appearing lesions composed of cells with high nuclear-to-cytoplasmic ratios and hyperchromatic nuclei arranged in nests and sheets, typically with peripheral palisading (Figs. 7.10 and 7.11). Nuclear atypia is more muted than in most non-keratinizing squamous cell carcinomas. Keratin pearls, if present at all, should be rare (Fig. 7.12) [10]. Some basaloid tumors infiltrate with an HSIL-like pattern that can masquerade as noninvasive disease, particularly given that basaloid tumors lack paradoxical maturation, one of the most useful signatures of invasion.

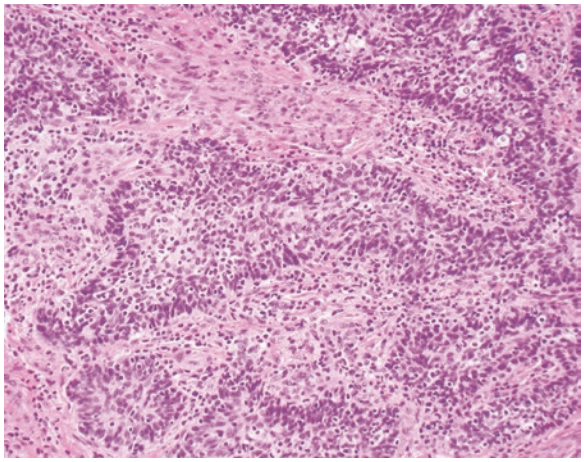

Fig. 7.10 Basaloid squamous cell carcinoma: Irregular malignant nests with peripheral palisading

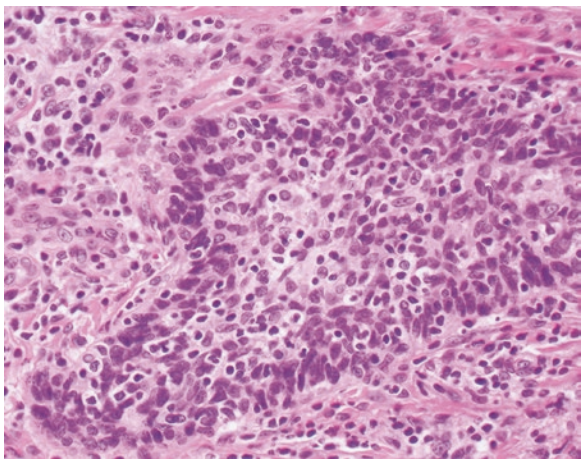

Fig. 7.11 Basaloid squamous cell carcinoma: Higher-power image of the case in Fig. 7.10, demonstrating peripheral palisading, high nuclear:cytoplasmic ratios, and minimal nuclear atypia

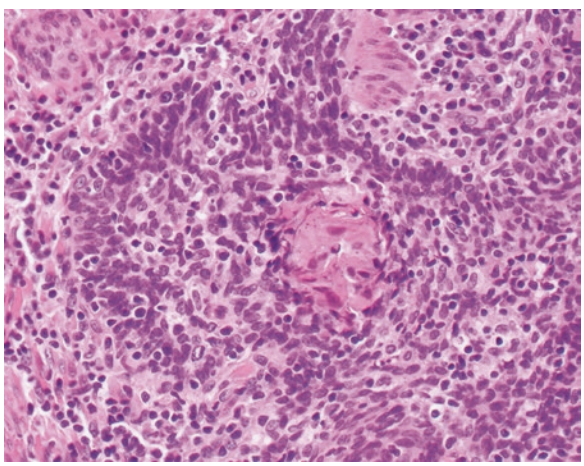

Fig. 7.12 Basaloid squamous cell carcinoma: Focal keratinization seen in the same case as in Figs. 7.10 and 7.11

7.4.1.4 Papillary Squamous Cell Carcinoma

Papillary squamous cell carcinoma comprises frond-like projections with fibrovascular cores (Fig. 7.13). The constituent cells show a hyperchromatic and basaloid appearance with frequent mitotic figures. Focal squamous maturation may be present, and multi-layering reminiscent of papillary urothelial tumors is typical (Fig. 7.14). Indeed, the term "papillary squamotransitional carcinoma" was historically applied to a subset of these cases, but that diagnosis has since fallen out of favor. The tumors that formerly fell into that category are now collapsed under the "papillary squamous cell carcinoma" umbrella [11–13].

Although clear invasion may be seen at the base of the lesion—sometimes in association with more conventional squamous cell carcinoma (Figs. 7.15 and 7.16)—it is not necessary to diagnose invasive carcinoma in this histologic subtype, as the architecture is consistent with the exophytic type of invasion. In practice, this means that a diagnosis of papillary squamous cell carcinoma can be rendered even in a superficial sample without visualization of the base, provided that the cytologic and architectural features fit. The morphologic differential includes giant condyloma, and the presence of low-risk HPV rather than high-risk HPV should raise suspicion for that entity [2].

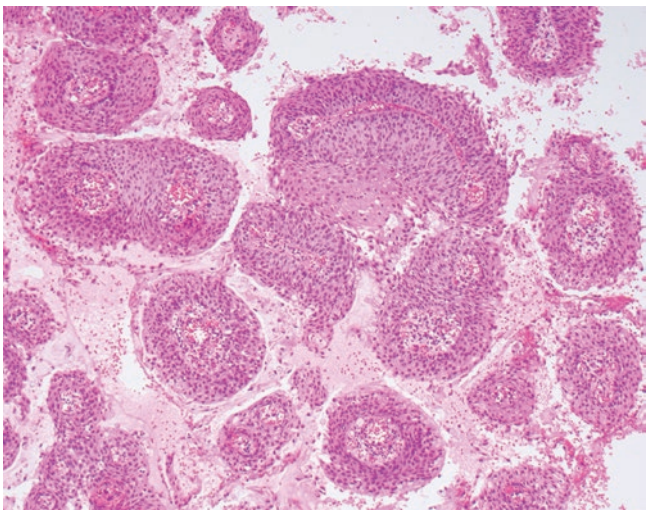

Fig. 7.13 Papillary squamous cell carcinoma: Frond-like projections with fibrovascular cores

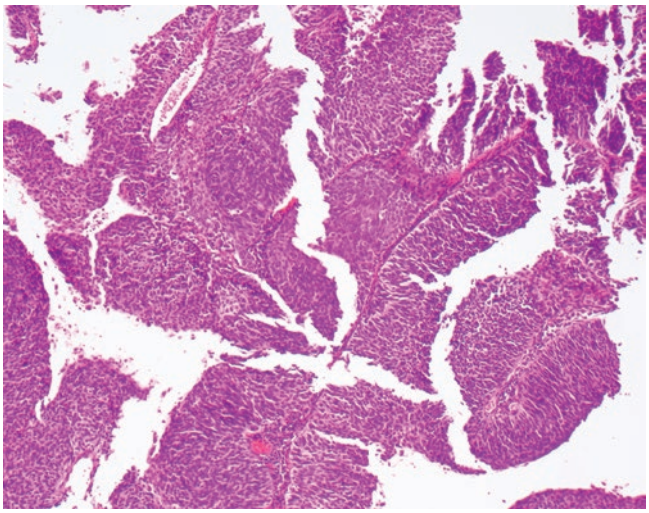

Fig. 7.15 Papillary squamous cell carcinoma: Superficial samplings of papillary squamous cell carcinoma do not typically demonstrate invasion and may provoke a differential of extensive HSIL, but a diagnosis of "carcinoma" can still be rendered in the context of this morphology

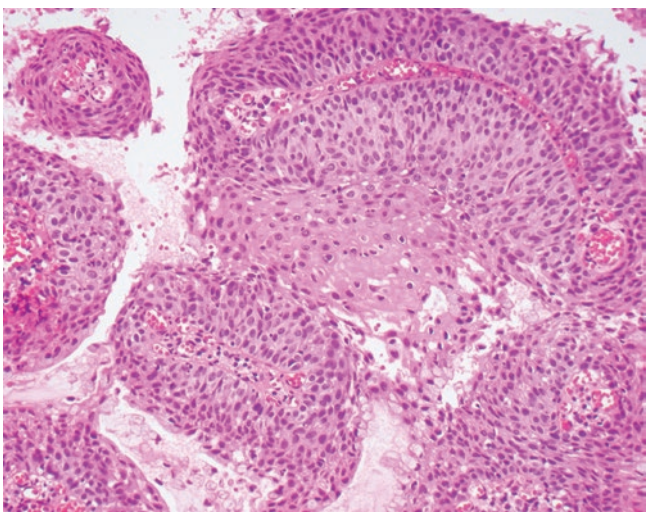

Fig. 7.14 Papillary squamous cell carcinoma: Higher-power view of the case depicted in Fig. 7.13, demonstrating a multi-layered epithelium reminiscent of urothelial-type differentiation

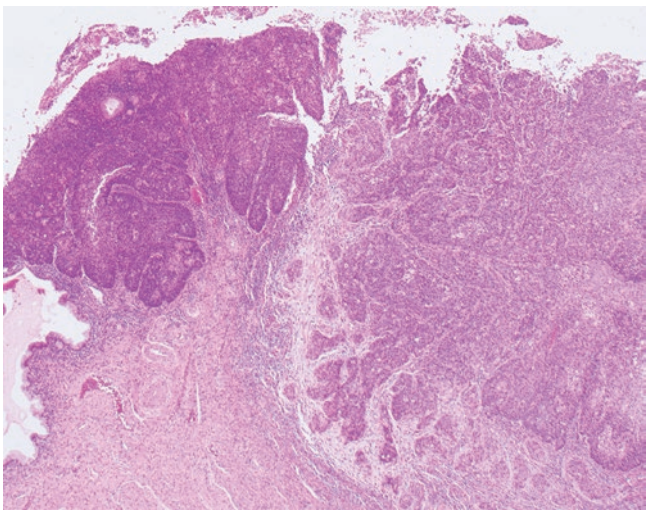

Fig. 7.16 Papillary squamous cell carcinoma associated with conventional squamous cell carcinoma: This case (lower-power view of the tumor depicted in Fig. 7.15) demonstrates papillary carcinoma on the left with associated conventional squamous cell carcinoma on the right

7.4.1.5 Warty-Type (Condylomatous) Squamous Cell Carcinoma

Warty-type squamous cell carcinoma shows exophytic, condylomatous architecture with koilocytic changes in the malignant cells, including cytoplasmic vacuolization and hyperchromatic nuclei. These lesions can be differentiated from condylomas by the presence of typical invasive squamous cell carcinoma morphology at the infiltrative edge. Warty-type squamous cell carcinoma is associated with multiple HPV subtypes, including both high-risk and low-risk subtypes, although the exclusive presence of low-risk types raises the possibility of a giant condyloma [14].

Notably, warty-type squamous cell carcinoma is not synonymous with "verrucous carcinoma," a variant of invasive carcinoma typified by blunt-edged infiltration and cytologic atypia restricted to the basal layers of epithelium and which primarily occurs in the vulva and the head and neck. Importantly, verrucous carcinomas are HPV-negative. The existence of this tumor in the cervix remains controversial, as most cases that have been categorized as such are HPV-positive and are, in retrospect, better classified as either condylomas or warty-type carcinomas [15, 16].

7.4.1.6 Lymphoepithelioma-like Carcinoma

Lymphoepithelioma-like carcinoma is composed of non-keratinizing, undifferentiated cells with large vesicular nuclei, prominent nucleoli, and moderate amounts of eosinophilic cytoplasm (Fig. 7.17). A marked infiltrate of lymphocytes, plasma cells, and eosinophils is characteristic, and the cell borders are typically indistinct and syncytial in appearance. Although Epstein-Barr virus drives carcinogenesis in similar-appearing tumors elsewhere, it does not appear to be involved in the pathogenesis of cervical lymphoepithelioma-like carcinoma; indeed, most of these tumors are HPV-associated [17, 18].

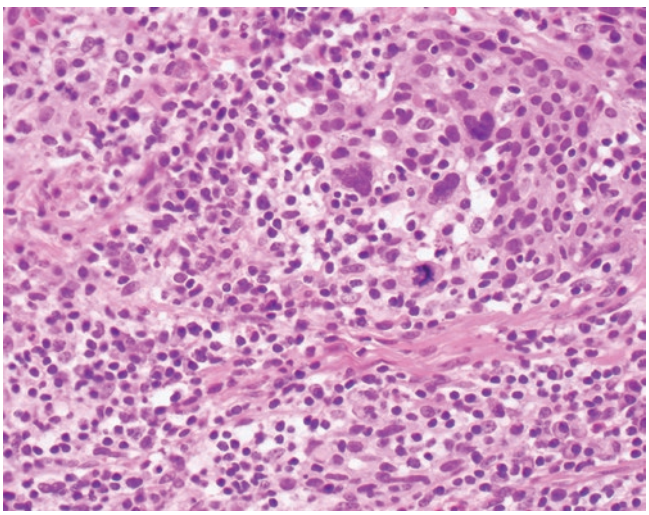

Fig. 7.17 Lymphoepithelioma-like squamous cell carcinoma: Non-keratinizing, undifferentiated cells with a loosely syncytial architecture and robust associated lymphoid infiltrate. Like other cervical squamous cell carcinomas, these tumors are associated with high-risk human papillomavirus (HPV) and show no etiologic link to Epstein-Barr virus

Diagnostic Highlights

- Tumor with multiple histologic subtypes that arises in association with HSIL
- Keratinizing subtype shows prominent polygonal cells with eosinophilic cytoplasm and keratohyalin granules, often with abnormal mitoses, keratin pearls, and saw-tooth infiltration
- Non-keratinizing subtype has marked pleomorphism and lack of keratin pearls and keratohyalin granules
- Basaloid subtype demonstrates muted cytologic atypia and lack of paradoxical maturation, making differentiation from HSIL difficult
- Papillary subtype has frond-like projections; requires distinction from giant condyloma by high-risk HPV positivity
- Warty-type subtype bears exophytic, condylomatous growth with conventional invasive squamous cell carcinoma at the infiltrative edge
- Lymphoepithelial-like subtype is characterized by undifferentiated cells and a marked inflammatory infiltrate driven by high-risk HPV (not Epstein-Barr virus as in other sites)

7.4.1.7 Cases

1. A 47-year-old woman with poorly differentiated squamous cell carcinoma (Figs. 7.2, 7.9, and 7.27)
2. A 53-year-old woman with superficially invasive squamous cell carcinoma demonstrating anaplasia and necrosis (Figs. 7.3, 7.4, 7.8, and 7.49)
3. A 60-year-old woman with keratinizing squamous cell carcinoma (Fig. 7.5)
4. A 51-year-old woman with keratinizing squamous cell carcinoma showing prominent keratinization and foreign-body giant cell reaction (Figs. 7.6 and 7.7)
5. A 66-year-old woman with keratinizing squamous cell carcinoma, basaloid subtype with a rare keratin pearl (Figs. 7.11 and 7.12)
6. A 33-year-old woman with a superficial biopsy of papillary squamous cell carcinoma (Figs. 7.13 and 7.14)
7. A 48-year-old woman with papillary squamous cell carcinoma in association with conventional squamous cell carcinoma (Figs. 7.15 and 7.16)
8. A 49-year-old woman with lymphoepithelioma-like carcinoma in a LEEP conization (Fig. 7.17)

7.4.2 Cytologic Appearance

Squamous cell carcinoma of the cervix manifests on cytologic preparations as atypical cells arranged singly and in clusters,

admixed with variable amounts of normal and dysplastic epithelium. The diagnostic cells show marked nuclear enlargement and coarse, irregular chromatin. Nucleoli may be prominent. Particularly helpful is the finding of so-called tadpole cells: single cells with markedly enlarged, atypical nuclei and moderate to abundant cytoplasm, showing an elongate, tapered cytoplasmic tail (Fig. 7.18). Orangeophilic, dyskeratotic cells are often prominent (Fig. 7.19). A component of HSIL may be notable in the background, and indeed, it can be difficult to impossible to distinguish between a basaloid squamous cell carcinoma and extensive HSIL on cytology. Classically, a prominent tumor diathesis with acute inflammation and necrotic debris is present; however, this may appear more muted on liquid-based preparations than on conventional preparations (Fig. 7.20).

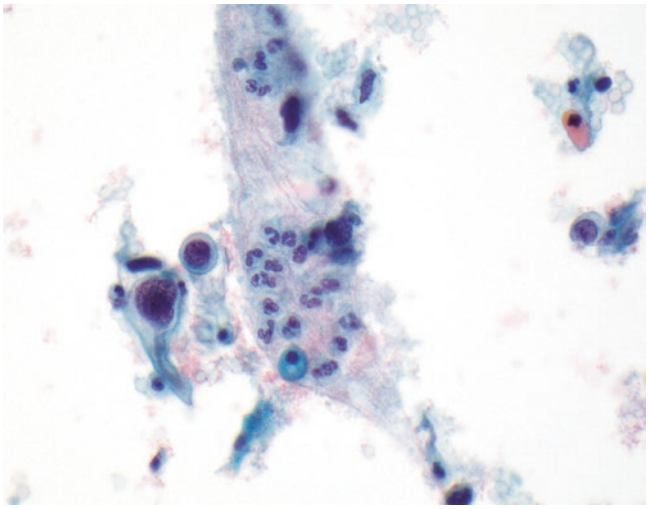

Fig. 7.18 Cervical squamous cell carcinoma cytology: Markedly atypical cells with enlarged, hyperchromatic nuclei. One cell (a "tadpole cell") shows abundant cytoplasm with a tapered, streaming tail

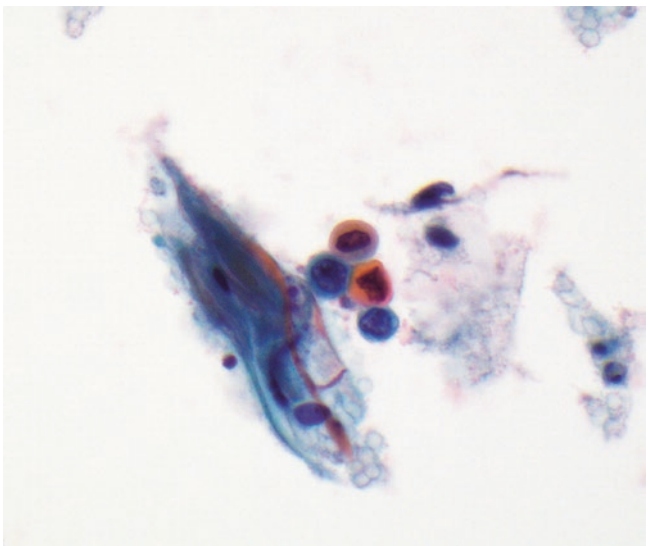

Fig. 7.19 Cervical squamous cell carcinoma cytology: Dyskeratotic cells with dense, orangeophilic cytoplasm and hyperchromatic nuclei are seen. Some show high nuclear:cytoplasmic ratios more typical of HSIL, whereas others show abundant streaming cytoplasm more typical of carcinoma

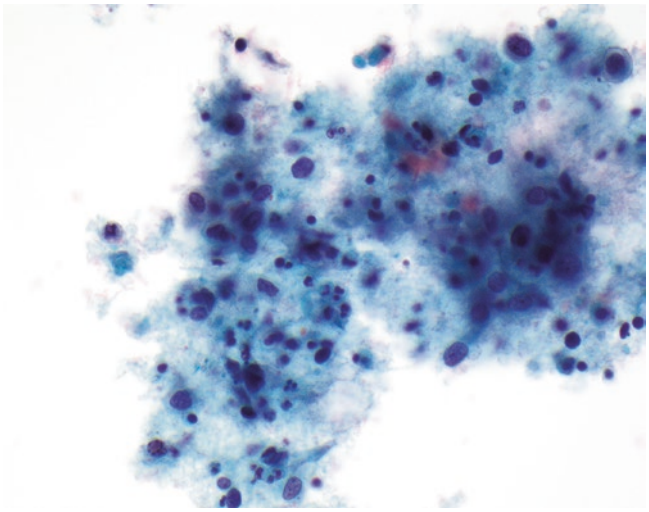

Fig. 7.20 Tumor diathesis cytology: A background of necrotic debris is typical of squamous cell carcinoma on cytology, but this finding may be more muted on liquid-based preparations (such as the ThinPrep illustrated here) than on conventional smears

Because many of the diagnostic features (streaming cells with abundant cytoplasm, sometimes prominent nucleoli, and decreased nuclear-to-cytoplasmic ratios relative to HSILs) can also be seen in reactive proliferations, the differential diagnosis may be a non-neoplastic process at first glance. Attention to nuclear size can quickly eliminate this possibility, however, as the constituent cells typically bear a nucleus that is at least five to ten times the size of a normal intermediate cell nucleus.

7.4.3 Grading Controversy

Squamous cell carcinoma of the cervix has historically been graded using some iteration of Broder's system, which assesses keratinization, cytologic atypia, and mitotic activity [19–21]. More recent versions also account for whether the invasive front of the tumor is pushing or infiltrative [22, 23]. Ultimately, however, none of the existing grading systems has proven reproducibly predictive of patient prognosis, and, as a result, tumor grading therefore currently has no significant clinical value for squamous cell carcinoma. It has been suggested that increased attention to tumor budding could improve the prognostic utility of cervical cancer grading, but this idea has not yet been codified in recommended grading systems [24–26]. The budding pattern of infiltration is discussed in further detail in Sect. 7.6.

7.4.4 Differential Diagnosis

When approaching a cervical biopsy or curettage, it is important to keep in mind that there are many entities to consider in the differential diagnosis of squamous cell carcinoma of the cervix.

- First, the possibility of a noninvasive lesion must be considered.
- Tangential sectioning is a commonly encountered difficulty when evaluating for the presence of invasion.
- Often the invasive nests will show features of paradoxical maturation, which is helpful but not sufficient for a diagnosis of invasion.
- Surrounding stromal responses including chronic inflammation and desmoplasia are additional supportive features, but HSIL also may attract a significant inflammatory response even in the absence of invasion.
- Deeper levels are often helpful in correcting for poor orientation [27]. Strategies for confirming the presence of invasion are discussed in further detail in Sect. 7.6.
- Other diagnoses to consider include reactive squamous changes (see Chap. 3), stromal decidual change, placental site nodule (see Chaps. 4 and 12), large cell and small cell neuroendocrine carcinoma (see Chap. 10), adenocarcinoma and adenosquamous carcinoma (see Chap. 8), melanoma (see Chap. 12), and changes associated with radiation therapy (see Chap. 3) (Table 7.1).

Table 7.1 Summary of the differential diagnosis of cervical squamous cell carcinoma

Differential Diagnosis	Histologic Features	Mitoses	Ki-67	CK	p63	p16	Other Positive Ancillary Studies
Cervical squamous cell carcinoma		Many	High	+	+	Diffuse	CK5/6, HPV-ISH
Decidual change	Low N:C, abundant pink cytoplasm	None/rare	Low	–	–	–/patchy	Vimentin, desmin, A1AT (cervical); CD10, ER (endometrial)
Placental site nodule	Irregular hyperchromatic nuclei, low N:C, hyalinized stroma	None/rare	<10%	+	+	–/patchy	Inhibin, focal hCG/hPL/ Mel-CAM, HLA-G
Epithelioid trophoblastic tumor	Irregular hyperchromatic nuclei, low N:C, hyalinized stroma	Few	10–20%	+	+	–/patchy	Inhibin, focal hCG/hPL/ Mel-CAM, HLA-G
Neuroendocrine carcinoma	Small round blue cells, irregular hyperchromatic nuclei, scant cytoplasm, apoptoses	Many	>90%	+ (perinuclear dot-like pattern)	–	Diffuse	Chromogranin, synaptophysin, CD56, panCK (dot-like), HPV-ISH
Adenocarcinoma	High N:C, fluffy cytoplasm, irregular chromatin and nuclear borders	Many	High	+	–	Diffuse	CK7, HPV-ISH
Adenosquamous carcinoma	Same as SCC but with admixed malignant glands. High N:C, fluffy cytoplasm, irregular chromatin and nuclear borders	Many	High	+	+	Diffuse	CK5/6, CK7, HPV-ISH
Melanoma	Variable appearance. Eccentric nuclei, prominent cherry-red nucleoli, vacuolated cytoplasm	Variable	High	–	–	Patchy or diffuse	S100, SOX-10, HMB45, Melan-A, MART-1, MIT-F.
Radiation change	Low N:C, bizarre nuclear atypia, smudgy chromatin	None/rare	Low	+	+	–/patchy	CK5/6

A1AT alpha-1-antitrypsin, *CK* cytokeratin, *ER* estrogen receptor, *hCG* human chorionic gonadotropin, *ISH* in situ hybridization, *N:C* nuclear-to-cytoplasmic ratio. *SCC* squamous cell carcinoma

7.4.4.1 Reactive Squamous Changes

Reactive epithelial atypia is one of the most commonly encountered findings on cervical biopsy. Acute and chronic inflammation can cause considerable nuclear atypia, including enlarged nuclei and prominent nucleoli. However, reactive squamous cells should not have the irregular nuclear contours, clumpy chromatin, and nuclear pleomorphism seen in HSIL and squamous cell carcinoma. Tangential sectioning can lead to a particularly worrisome appearance, with the illusion of infiltration in such cases. Deeper levels and ancillary studies such as p16 immunohistochemistry are usually sufficient to distinguish between reactive atypia and HSIL/squamous cell carcinoma. (See Sect. 7.5 below, Ancillary Studies.)

7.4.4.2 Decidual Change

Cervical decidual change (deciduosis) is a hormone-related change in the cervical stroma during pregnancy that can mimic squamous neoplasia both clinically and histologically [28, 29]. The lower uterine segment may also show pseudodecidual change in the context of exogenous hormone therapy, and it is often sampled on endocervical curettage. In both cases, the stromal cells become plump, with abundant eosinophilic cytoplasm, round nuclei, fine chromatin, and prominent nucleoli. Importantly, however, significant cytologic atypia and mitotic activity should be absent. Immunohistochemistry may be helpful in addressing this differential, as both cervical and endometrial deciduosis lack cytokeratin and p63 expression and show either negative or only patchy p16 expression. Cervical deciduosis is positive for vimentin, desmin, and alpha-1-antitrypsin, and decidualized endometrium is CD10 and ER positive.

7.4.4.3 Placental Site Nodule and Epithelioid Trophoblastic Tumor

Placental site nodules are not infrequently encountered in endometrial and endocervical curettage specimens. They can occur many years after a pregnancy and are typically identified as an incidental finding associated with endometrial sampling [30]. Placental site nodules are nodular in appearance and are composed of large, atypical mononuclear trophoblastic cells embedded within a hyalinized stroma, often with a densely hyalinized, acellular center (Figs. 7.21 and 7.22). Mitotic figures are usually not identified.

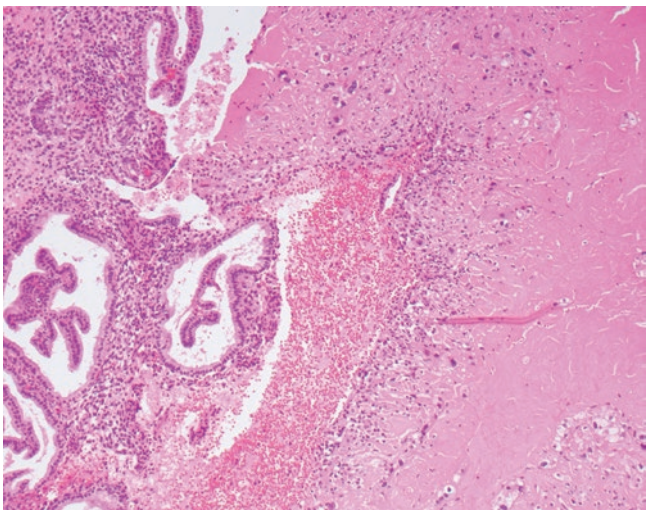

Fig. 7.21 Placental site nodule: Arising in close association with the endometrium, placental site nodules have a densely hyalinized center appreciable from low power

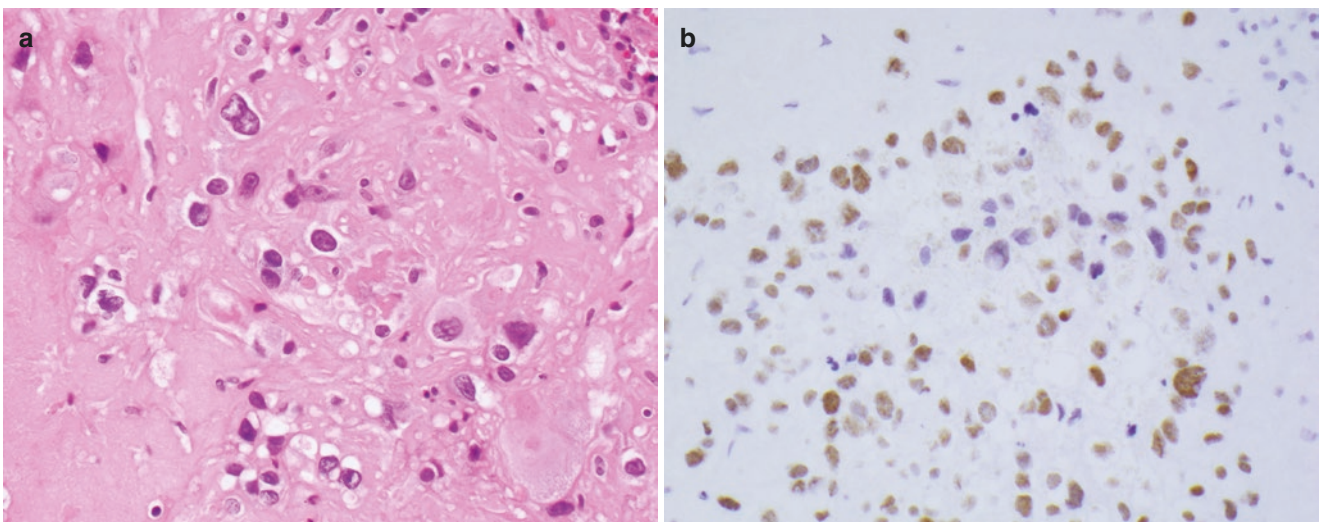

Fig. 7.22 Placental site nodule: The constituent cells are atypical but lack mitotic activity (**a**). p63 is strongly positive (**b**), provoking possible confusion with squamous cell carcinoma

The malignant counterpart of a placental site nodule is the epithelioid trophoblastic tumor. This type of gestational trophoblastic disease can deeply invade the myometrium and cervical stroma. Cases may occur after a long latent period after gestation, and approximately half of cases present in the lower uterine segment or cervix [30, 31]. In a small sampling, epithelioid trophoblastic tumor has many morphologic similarities with placental site nodule: both are composed of chorionic-type intermediate trophoblastic cells with irregular, hyperchromatic nuclei and abundant eosinophilic cytoplasm, with a background of hyalinized stroma. Epithelioid trophoblastic tumors, however, often bear large areas of geographic necrosis, which may or may not be sampled in a curettage specimen (Figs. 7.23 and 7.24). Taken in concert with the nested growth pattern, distinct cell borders, and abundant eosinophilic cytoplasm, this necrosis can closely mimic squamous malignancy [32]. In addition, the lesional cells can colonize the cervical squamous epithelium, masquerading as HSIL [33]. Thus, the apparent presence of an associated intraepithelial lesion does not exclude the possibility of an epithelioid trophoblastic tumor.

Confusion with squamous cell carcinoma is amplified by the fact that both epithelioid trophoblastic tumors and placental site nodules are strongly positive for p63 and cytokeratins (see Fig. 7.22). In contrast to squamous cell carcinoma, however, they can also express inhibin with focal hPL and beta-hCG. The most discerning marker for this differential, however, is p16, which is negative or shows only patchy expression in both trophoblastic proliferations, whereas diffuse, strong positivity is typical of cervical squamous cell carcinoma [34].

7.4.4.4 Neuroendocrine Carcinoma

Neuroendocrine carcinoma can also mimic squamous cell carcinoma of the cervix, particularly those with basaloid features. Both small cell neuroendocrine carcinoma and large cell neuroendocrine carcinoma of the cervix have a strong association with high-risk HPV, with a predominance of HPV type 18 particularly in small cell neuroendocrine carcinoma [35]. Small cell neuroendocrine carcinomas display sheet-like proliferations of cells with monotonous, medium-sized hyperchromatic nuclei with stippled chromatin, nuclear molding, inconspicuous nucleoli, and scant cytoplasm (Fig. 7.25). Apoptotic bodies and mitotic figures are abundant. Large-cell neuroendocrine carcinoma has larger nuclei, prominent nucleoli, and more abundant cytoplasm.

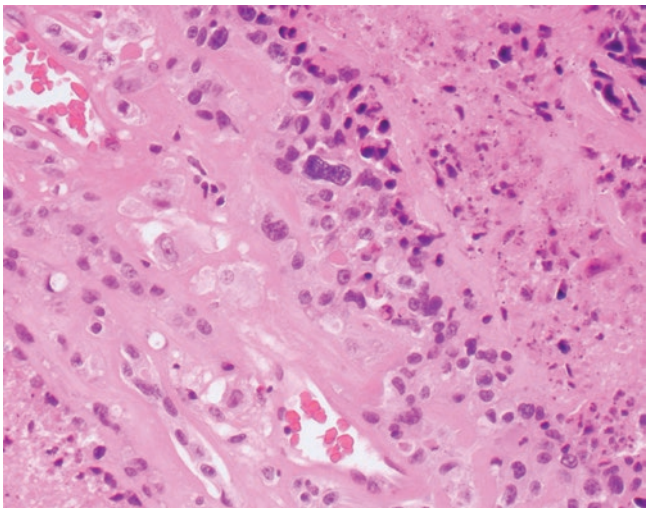

Fig. 7.24 Epithelioid trophoblastic tumor: Necrosis is highlighted in this higher-power view of the same case depicted in Fig. 7.23. This tumor was metastatic to the liver

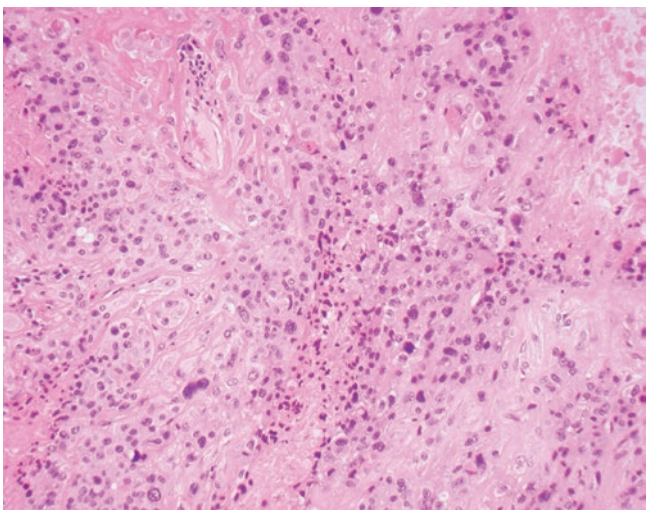

Fig. 7.23 Epithelioid trophoblastic tumor: The cytomorphology and associated hyalinization is reminiscent of placental site nodule, but prominent necrosis is also present

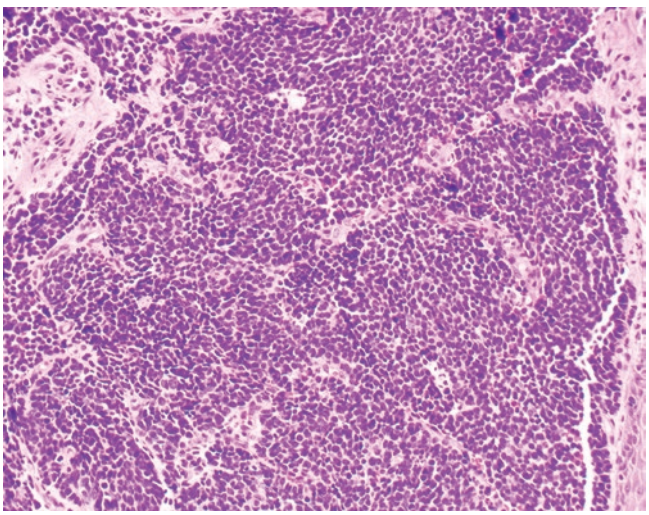

Fig. 7.25 Small cell neuroendocrine carcinoma: Sheet-like proliferation of cells with monotonous ovoid nuclei and minimal associated cytoplasm. At low-power, this tumor invokes a differential of basaloid and poorly differentiated non-keratinizing squamous cell carcinoma

Although these tumors are morphologically distinct from keratinizing squamous cell carcinoma, they show overlapping features with basaloid and poorly differentiated nonkeratinizing squamous cell carcinomas. A panel that includes neuroendocrine markers (such as synaptophysin, chromogranin, and CD56), as well as markers for squamous differentiation (such as p63 and CK5/6), can be useful in this setting (Figs. 7.26 and 7.27) Note that neuroendocrine tumors are expected to show both strong p16 expression and high-risk HPV positivity, so these studies have no value in resolving this differential. It is important to distinguish neuroendocrine carcinoma from squamous cell carcinoma because the prognosis appears to be considerably worse for neuroendocrine tumors, and treatment approaches—though not well codified for neuroendocrine carcinomas in the cervix—may vary [36].

7.4.4.5 Adenocarcinoma/Adenosquamous Carcinoma, Including Glassy Cell Carcinoma

Though less commonly encountered than squamous cell carcinoma, adenocarcinoma and adenosquamous carcinoma of the cervix also enter into the differential. Both entities are associated with high-risk HPV, most notably type 16 and (to a greater extent than in squamous cancer) type 18 [37, 38]. Adenocarcinoma can be particularly challenging to recognize when well-formed glands are absent and the tumor instead assumes confluent, sheet-like architecture (Fig. 7.28). The absence of intercellular bridges and keratinization are helpful clues suggestive of adenocarcinoma, but these features are not always evident in basaloid or poorly differentiated squamous cell carcinoma either. Immunohistochemistry for CK5/6 and p63 can help clarify the diagnosis, as these markers should be strongly positive in squamous cancer but absent in adenocarcinoma. CK7 also may be of use because, though it is often positive in squamous cancer, it typically shows more diffuse and strong staining in adenocarcinoma [39].

Adenosquamous carcinoma of the cervix is characterized by well-defined squamous and glandular elements (Fig. 7.29). Thorough sampling is necessary to ensure adequate representation of both components of this tumor. Glassy cell carcinoma has been considered to be a poorly differentiated variant of adenosquamous carcinoma and has been associated with HPV18 infection [30, 40]. More recent work has demonstrated that this entity is rather a poorly differentiated type of invasive adenocarcinoma. Morphologically, glassy cell carcinoma has abundant eosinophilic cytoplasm with a "ground glass" appearance, distinct cell borders, large round nuclei, and prominent nucleoli.

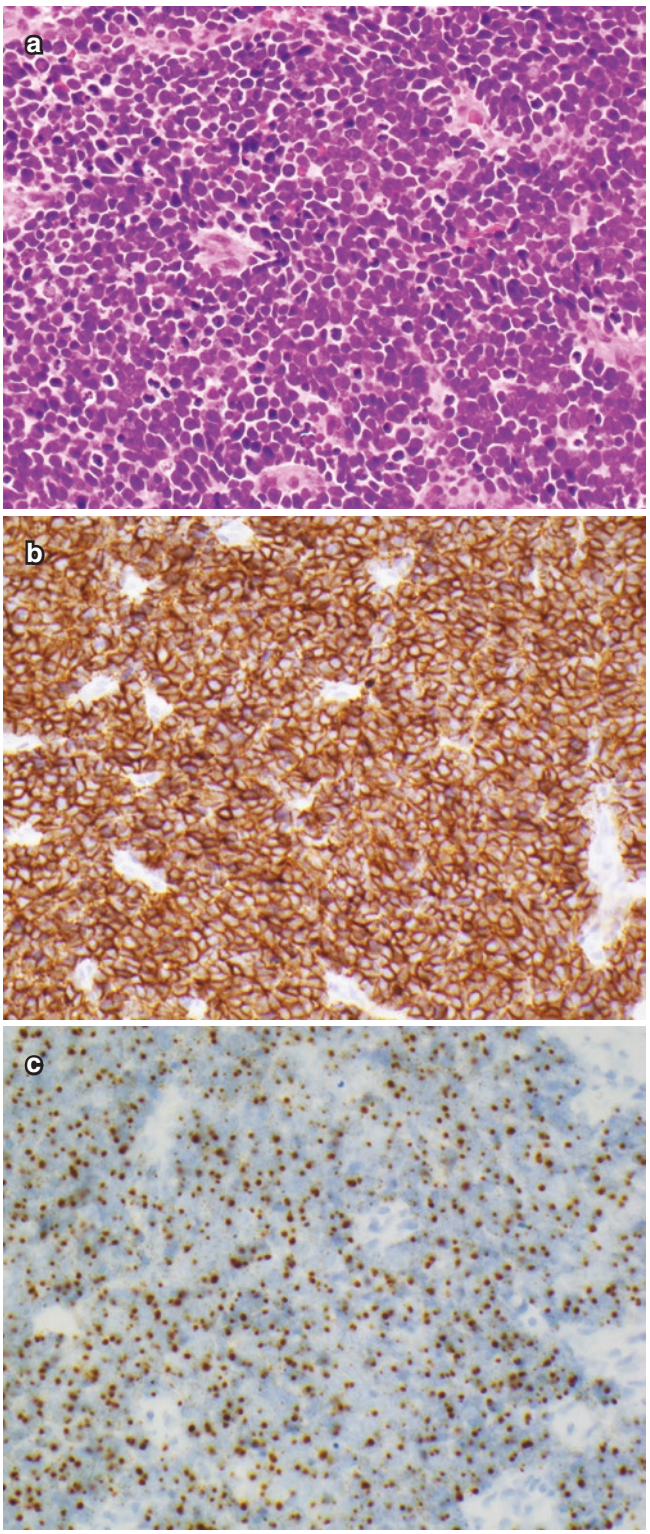

Fig. 7.26 Small cell neuroendocrine carcinoma: A higher-power view of the same case depicted in Fig. 7.25 reveals stippled chromatin and nuclear molding typical of small cell carcinoma (**a**). The diagnosis is further supported by strong diffuse CD56 immunostaining (**b**). Like squamous cell carcinomas, these tumors are predominantly driven by high-risk HPV, illustrated here as punctate staining for high-risk HPV E6/E7 mRNA on in situ hybridization (**c**)

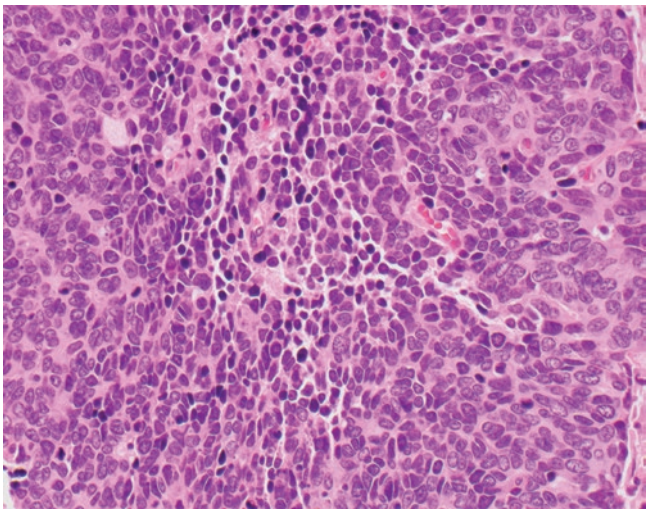

Fig. 7.27 Non-keratinizing squamous cell carcinoma with small cell-like features: This squamous cell carcinoma closely mimics small cell carcinoma with its enlarged nuclei, scant cytoplasm, chromatin stippling, and suggestion of nuclear molding. Performing neuroendocrine and squamous markers is prudent in such cases to ensure proper classification

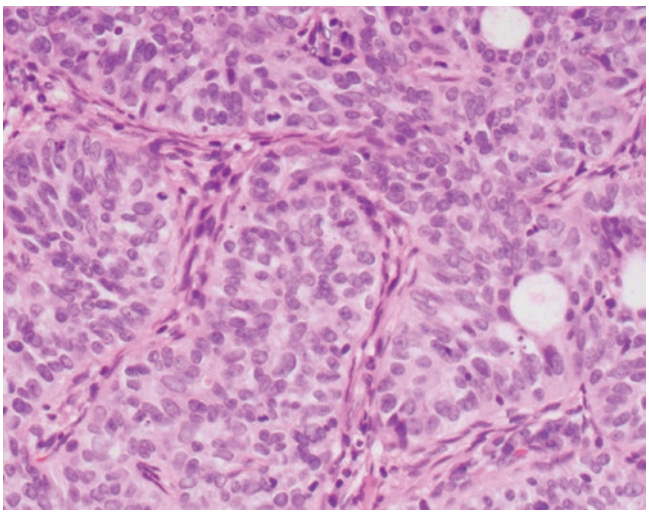

Fig. 7.28 Adenocarcinoma: Focal gland formation helps secure the diagnosis of adenocarcinoma in this case, but the solid-appearing areas on the left-hand side of the image illustrate how it can sometimes be difficult to differentiate between adenocarcinoma and squamous cell carcinoma

7.4.4.6 Melanoma

Malignant melanoma can be primary or metastatic to the cervix and should always be considered in the differential of a poorly differentiated malignancy of the cervix. Immunohistochemistry for cytokeratins, p63, and melanocytic markers including HMB-45, Melan-A, S100, and SOX-10 should be sufficient to identify melanoma. p16 has been reported to have a variety of expression patterns in melanoma [41], so it is not a useful marker to distinguish melanoma from squamous cell carcinoma, nor does it imply HPV association.

7.4.4.7 Other Carcinomas

Poorly differentiated carcinomas from other locations, including the endometrium, the ovary, and the bladder, can sometimes mimic squamous cell carcinoma of the cervix. In this setting, lineage-specific markers and direct HPV testing are prudent, as p16 can be positive in a host of cancers outside the cervix that are not associated with HPV [42–44]. For more detail on ancillary studies, see Sect. 7.5.

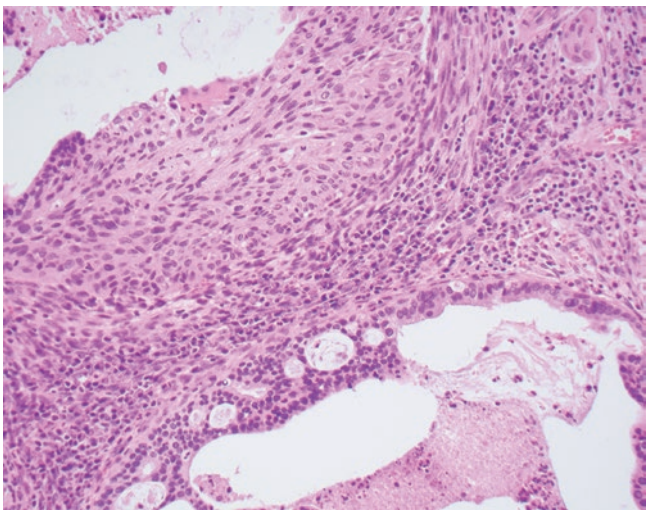

Fig. 7.29 Adenosquamous carcinoma: This diagnosis requires the juxtaposition of obvious and distinct squamous cell carcinoma (*upper left*) and adenocarcinoma (*lower right*) elements

7.4.4.8 Radiation Changes

Pelvic radiation therapy can result in marked cytologic atypia of ectocervical and endocervical mucosa and the underlying

stroma, which may provoke consideration for recurrent or residual squamous cell carcinoma (Figs. 7.30, 7.31, 7.32). Clues to a diagnosis of benign radiation-associated change include the constellation of bizarre cytologic atypia with smudgy, degenerative-appearing chromatin, enlarged nuclei but low nuclear-to-cytoplasmic ratios, and no appreciable mitotic activity.

Direct testing for high-risk HPV can be useful for distinguishing treatment effect from recurrent squamous cell carcinoma. Additionally, cytokeratin staining may be useful when assessing for the differential of radiation-associated stromal atypia *versus* squamous cell carcinoma; however, it must be interpreted with care, as reactive fibroblasts can show non-specific keratin staining. Caution should also be used when applying p16 in this context, as radiation-associated benign atypia can be strongly p16-positive [45]. Of note, if a new radiation-induced cervical or vaginal cuff squamous cell carcinoma is suspected, p16 and high-risk HPV will not be able to distinguish a non–HPV-driven squamous cell carcinoma from radiation change.

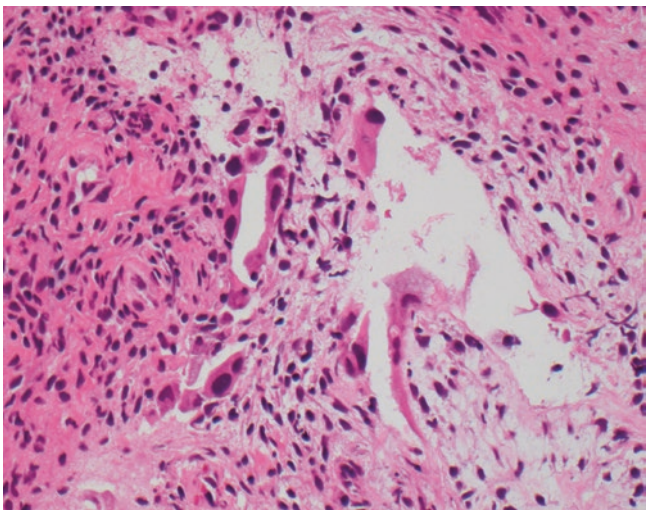

Fig. 7.31 Radiation atypia in endocervical glands: Benign endocervical glands can show prominent radiation-associated change, with increased eosinophilic cytoplasm that suggests squamous differentiation. Importantly, these cells may be p16-positive, so that stain should be used and interpreted with extreme caution in the context of prior radiotherapy

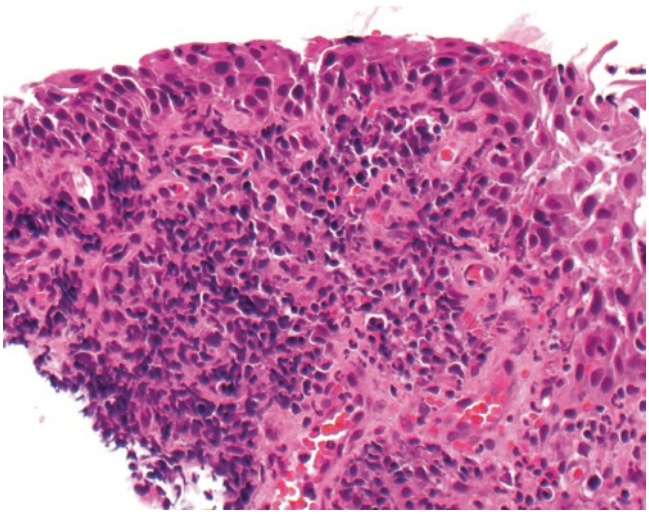

Fig. 7.30 Radiation atypia: Radiation treatment results in cytologic atypia that can mimic squamous cell carcinoma. Here the surface epithelium and underlying stroma demonstrate nuclear hyperchromasia and enlargement that provoke a malignant differential. Importantly, nuclear enlargement is accompanied by increased cytoplasm, and the quality of the chromatin is smudgy and degenerative rather than coarse

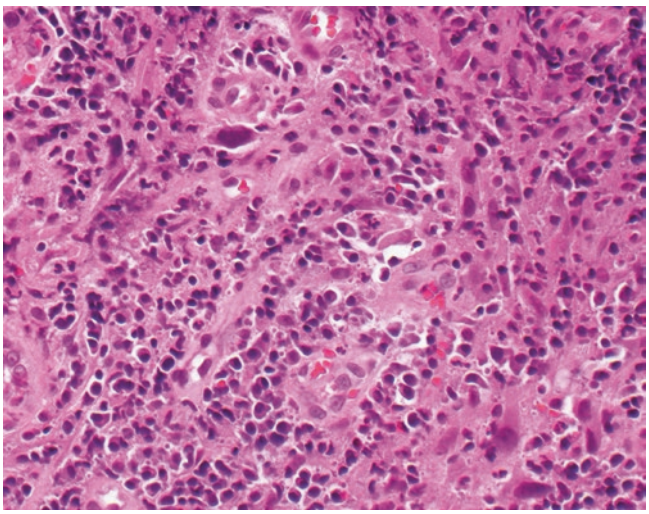

Fig. 7.32 Radiation atypia in stromal cells: Stromal cells classically show hyperchromasia and enlargement following radiotherapy. Here they are associated with necroinflammation, which further suggests a possible malignant diagnosis. Cytokeratin staining may be reassuring in this context, although care must be taken not to mistake non-specific fibroblast staining for epithelial differentiation

Diagnostic Highlights

- Many benign and malignant entities can mimic squamous cell carcinoma of the cervix, including reactive squamous atypia, radiation atypia, decidual change, trophoblastic proliferations, cervical adenocarcinomas and neuroendocrine carcinomas, and malignancies arising from other organs. Placental site nodule and epithelioid trophoblastic tumor have a squamoid appearance and express p63. Always perform p16 immunohistochemistry when trying to exclude these mimickers.
- Radiation-associated benign atypia can be p16-positive.

7.4.4.9 Cases

1. A 36-year-old woman with a placental site nodule (Figs. 7.21 and 7.22)
2. A 35-year-old woman with an epithelioid trophoblastic tumor (Figs. 7.23 and 7.24)
3. A 54-year-old woman with small cell neuroendocrine carcinoma (Figs. 7.25 and 7.26)
4. A 50-year-old woman with adenosquamous carcinoma (Fig. 7.28)
5. A 52-year-old woman with adenosquamous carcinoma (Figs. 7.29)
6. A 36-year-old woman with history of squamous cell carcinoma who received radiation therapy (Figs. 7.30, 7.31, 7.32)

7.5 Ancillary Studies

Although cervical squamous cell carcinoma is usually a morphologic diagnosis, ancillary studies can be valuable for excluding entities on the differential in challenging cases.

7.5.1 p16

Immunohistochemistry for p16 is the most commonly utilized ancillary test for the detection of high-risk HPV-related lesions in the gynecologic tract. The tumor suppressor p16 functions as a cyclin-dependent kinase inhibitor and plays an important role in cell cycle regulation. The HPV viral oncoprotein E7 targets the retinoblastoma (Rb) tumor suppressor protein for degradation and upregulates p16, leading to dysregulation of the cell cycle. This virally induced upregulation of p16 can be reliably detected via immunohistochemistry [46]. Use of p16 immunohistochemistry has been shown to increase interobserver agreement among pathologists making diagnoses of squamous intraepithelial neoplasia, and strong, diffuse (>70%) nuclear +/− cytoplasmic expression can be used to confirm an HPV-driven malignancy in the setting of invasive cervical squamous cancer (Fig. 7.33) [47, 48].

It is important to exercise caution, however, when interpreting this marker if the differential includes high-grade malignancies from other sites of origin—including the endometrium, ovary, and bladder—as these tumors may show high levels of p16 expression unrelated to HPV [42–44]. For instance, p16 is commonly overexpressed in endometrial serous carcinomas that are unaffiliated with HPV [44]. Furthermore, other histotypes of HPV-driven cervical cancer—including adenocarcinomas and small cell carcinomas—show strong, diffuse p16 staining. Thus, p16 has high sensitivity for squamous cell carcinoma only in the correct anatomic and morphologic context.

p16 also has minor sensitivity shortcomings in the diagnosis of cervical squamous cancer because of its failure to high-

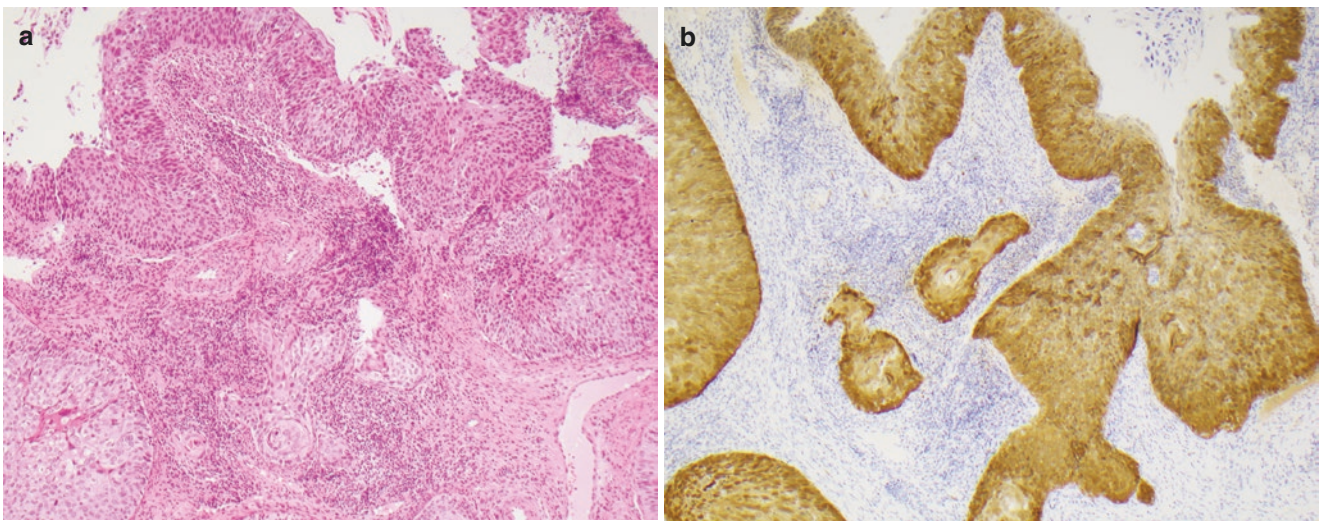

Fig. 7.33 p16 in cervical squamous carcinoma: The vast majority of cervical squamous carcinomas—including the one depicted here (**a**)—will be strongly and diffusely positive for p16 (**b**), which serves as a reliable surrogate for HPV infection in this morphologic and anatomic context

light a small subset of cases. Although more than 95% of cervical squamous cell carcinomas are attributable to high-risk HPV infection, the rare HPV-negative cases show only patchy p16 expression rather than the diffuse staining characteristic of HPV-associated tumors [49, 50]. Additionally, squamous cell carcinoma associated with high-risk HPV occasionally will lose p16 expression entirely; this represents another setting where direct HPV testing may be useful (Fig. 7.34).

7.5.2 HPV DNA and RNA In Situ Hybridization

Direct detection of HPV sometimes may be important for diagnosing cervical squamous cell carcinoma, owing to the previously mentioned shortcomings of p16 immunohistochemistry in some contexts. HPV DNA in situ hybridization was the initial assay developed for direct HPV testing on formalin-fixed, paraffin-embedded tissue samples, but this assay is no longer clinically utilized. Testing for high-risk HPV E6/E7 RNA by in situ hybridization has since supplanted this test because of its high sensitivity and specificity for transcriptionally active HPV [51, 52].

Using high-risk HPV polymerase chain reaction (PCR) as the gold standard, high-risk HPV mRNA E6/E7 in situ hybridization has a 98% sensitivity for the detection of high-risk HPV-related neoplasia [51]. A positive signal appears as punctate staining centered in the cytoplasm and, to a lesser extent, overlying the nuclei. Occasionally, evaluation of multiple fields with high-power magnification is required for identification of sparse staining, but this is rarely necessary; invasive cancers typically show a high viral burden readily appreciable from medium power, although it may not always be obvious at low power (Fig. 7.35) [51].

High-risk HPV E6/E7 mRNA in situ hybridization may be particularly valuable in cases that are clearly squamous but are p16-negative or equivocal, as well as in high-grade cancers where the differential includes alternative histotypes and sites of origin for which strong p16 staining does not necessarily suggest HPV infection.

Diagnostic Highlights

- p16 is a strong surrogate marker for high-risk HPV infection in the cervix, but it has minor sensitivity and specificity issues.
- HPV E6/E7 RNA in situ hybridization is a highly sensitive and specific marker for transcriptionally active HPV and may be useful when p16 immunohistochemistry results are confounding or if the differential includes non-cervical sites of origin.
- Strong, diffuse p16 expression is not necessarily evidence for squamous cancer associated with high-risk HPV if the differential diagnosis includes malignancies from other anatomic sites and/or other HPV-associated tumor types.

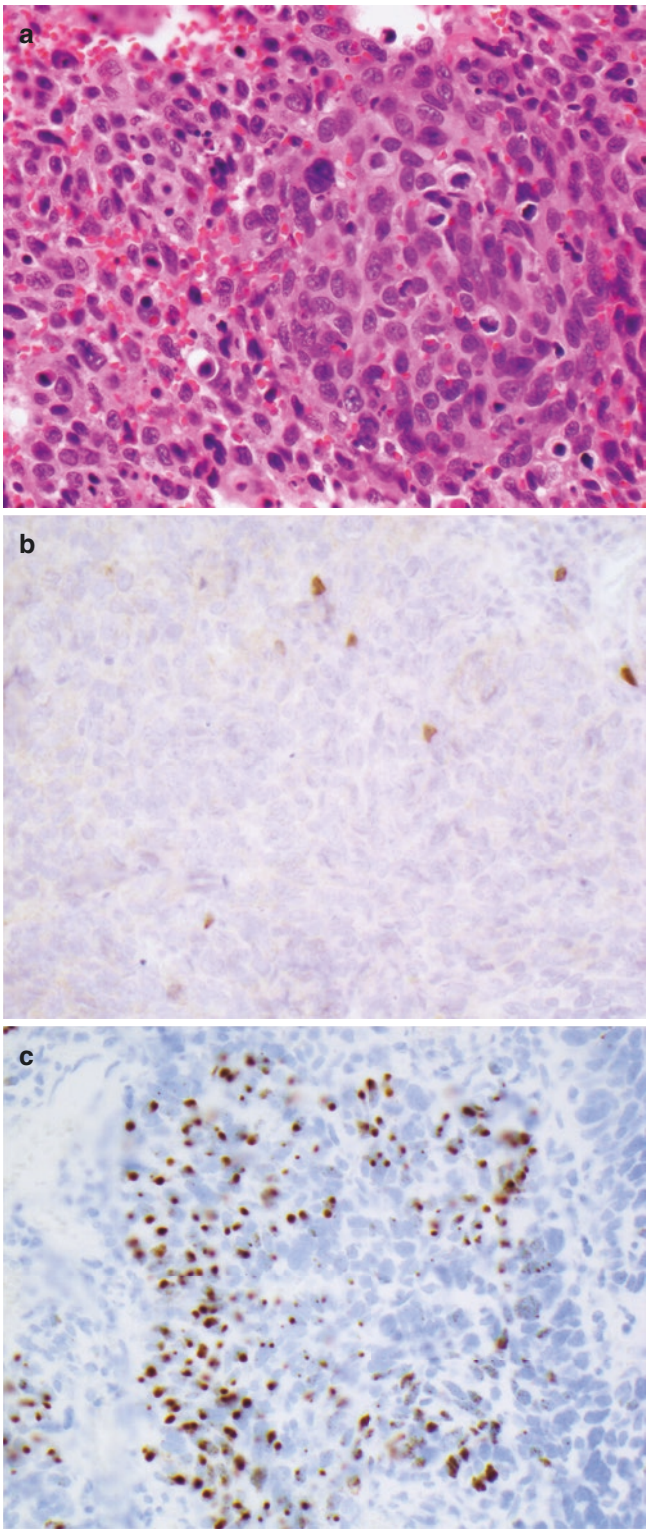

Fig. 7.34 p16-negative HPV-associated squamous cell carcinoma: In this rare case of squamous cell carcinoma (**a**), p16 expression has been lost (**b**). The presence of high-risk HPV E6/E7 mRNA by in situ hybridization shows that it is clearly HPV-associated (**c**)

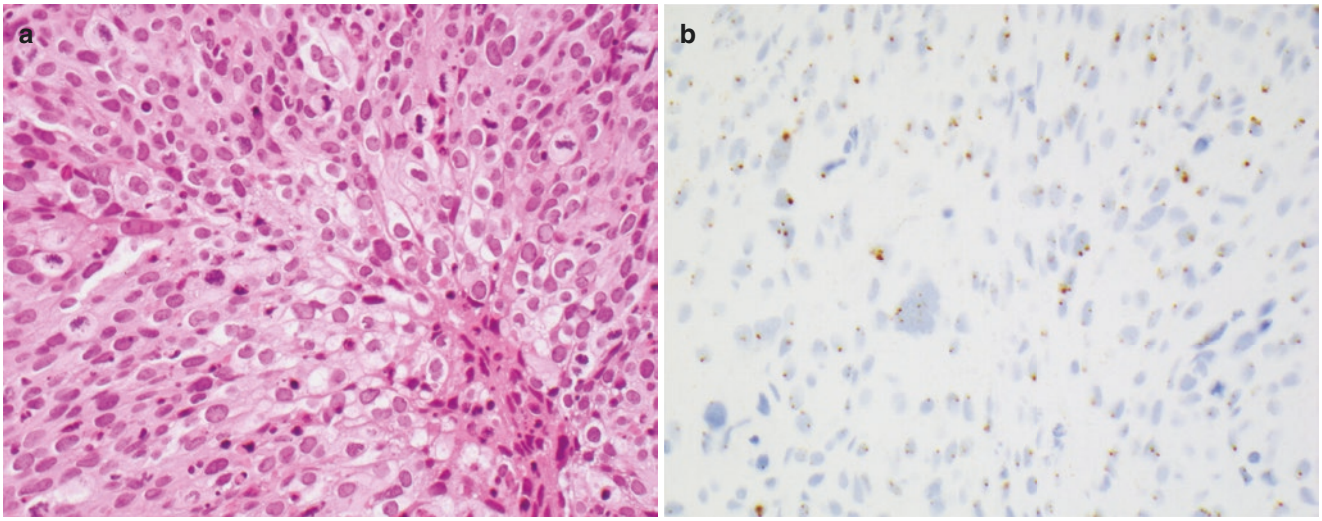

Fig. 7.35 HPV RNA in situ hybridization: This squamous cell carcinoma (**a**) shows punctate staining for high-risk HPV E6/E7 RNA (**b**). The positive signals appear both in the cytoplasm and overlying the nuclei. Note that expression is less obvious than in the case depicted in Fig. 7.34, emphasizing the fact that evaluation may require medium-power or even high-power assessment to avoid missing focal positive signals

7.5.3 Cases

1. A 41-year-old woman with p16-negative, HPV-associated squamous cell carcinoma (Fig. 7.34)
2. A 28-year-old woman with endocervical involvement by HSIL (Fig. 7.37).

7.6 Assessing Depth of Invasion

7.6.1 Challenges with Assessing Depth of Invasion

The accurate identification of stromal invasion is critical for the proper diagnosis, staging, and management of cervical squamous neoplasia. This can be particularly challenging for cases with only focal and limited infiltration beyond the basement membrane. First, tangential sectioning or endocervical extension of HSIL must be excluded. It is important to note that numerous bulky, deep nests of neoplastic squamous epithelium can occur in the setting of extensive endocervical gland extension by HSIL (Figs. 7.36 and 7.37). In such cases, the immature appearance, rounded contours of the lesional nests, absence of a prominent desmoplastic stromal response, and distribution aligned with normal endocervical glands help exclude invasion.

When compared with the cells in overlying intraepithelial lesions, invasive cells often demonstrate more vesicular chromatin, more pleomorphic nuclei, and nucleoli that are more prominent. One of the most useful clues to the presence of invasion is paradoxical maturation, which is typified by the accumulation of eosinophilic cytoplasm (Figs. 7.38 and 7.39). This richly eosinophilic appearance contrasts with the basaloid hue of background intraepithelial lesions and is often the best low-power clue that the lesion has progressed to invasive carcinoma. Notably, however, the basaloid subtype of invasive carcinoma will lack this feature and therefore may be more challenging to distinguish from overlying HSIL (Fig. 7.40).

A stromal reaction also can be helpful, as invasion is typically associated with a desmoplastic stromal response and/or a robust lymphoid reaction (Figs. 7.41 and 7.42). It is important to note, however, that intraepithelial lesions also may show a prominent underlying lymphoid response, and its presence does not dictate the diagnosis of invasion.

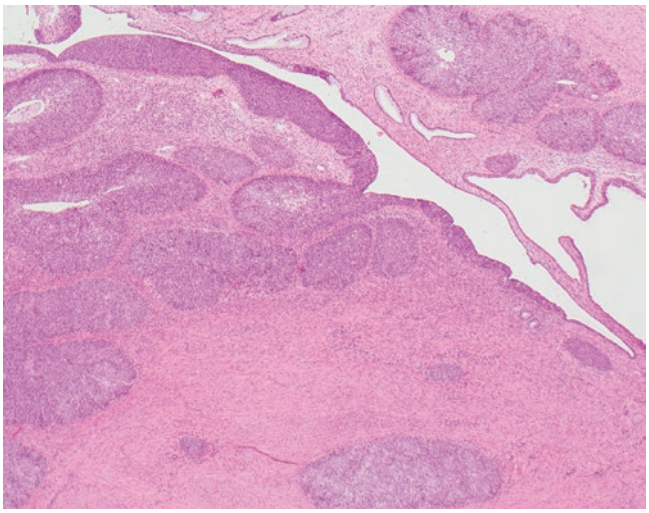

Fig. 7.36 High-grade squamous intraepithelial lesion (HSIL): HSIL may show bulky extension into endocervical glands, mimicking invasive squamous cell carcinoma. Careful assessment for associated desmoplasia, paradoxical maturation, and extension beyond the normal endocervical gland distribution is required to exclude invasion in such cases

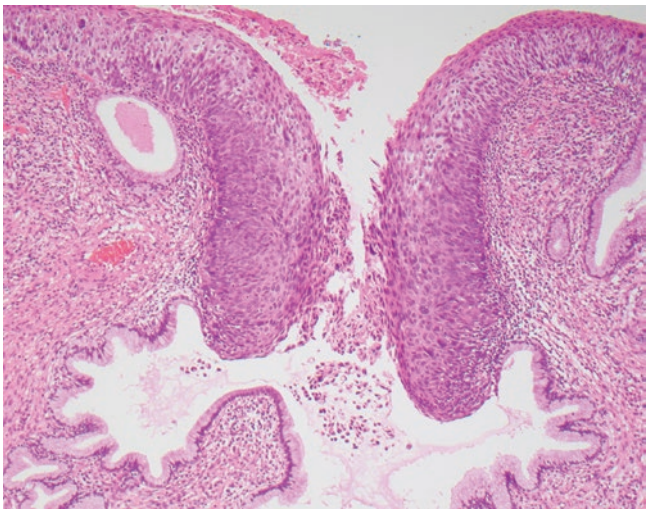

Fig. 7.37 High-grade squamous intraepithelial lesion (HSIL): This higher-power view of the case depicted in Fig. 7.36 shows an area with early extension of HSIL into an endocervical gland

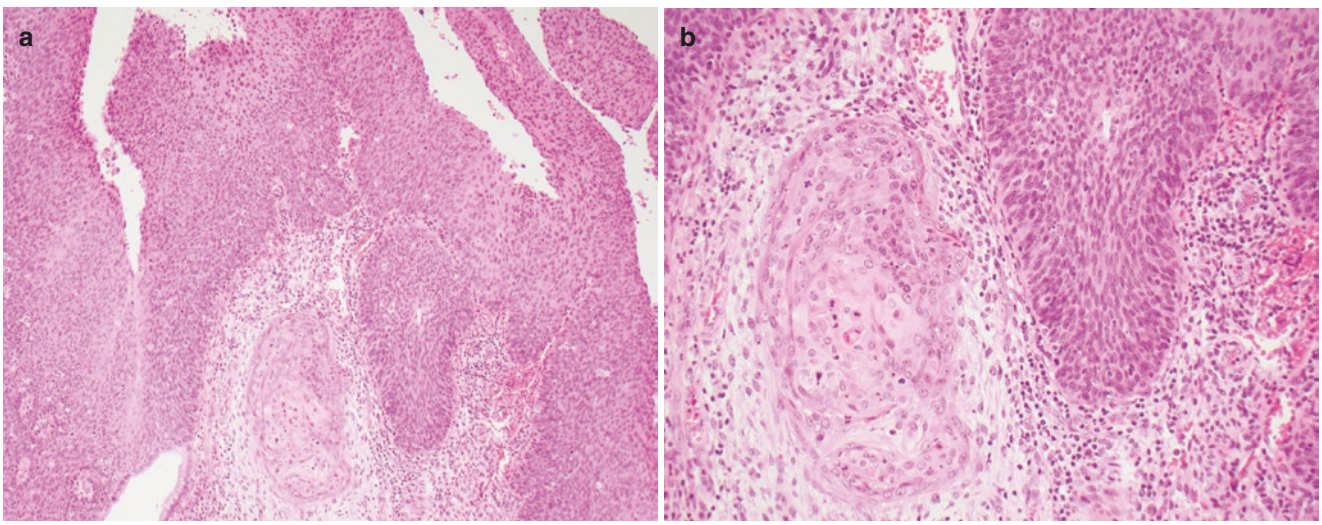

Fig. 7.38 Paradoxical maturation: The abrupt accumulation of eosinophilic cytoplasm is useful for identifying focal invasion associated with overlying intraepithelial neoplasia. This case (**a**) shows a nest of invasion that sharply contrasts with the more basaloid adjacent high-grade squamous intraepithelial neoplasia (**b**, higher power). Note that prominent desmoplasia is also seen in association with the invasive area but is absent next to the HSIL

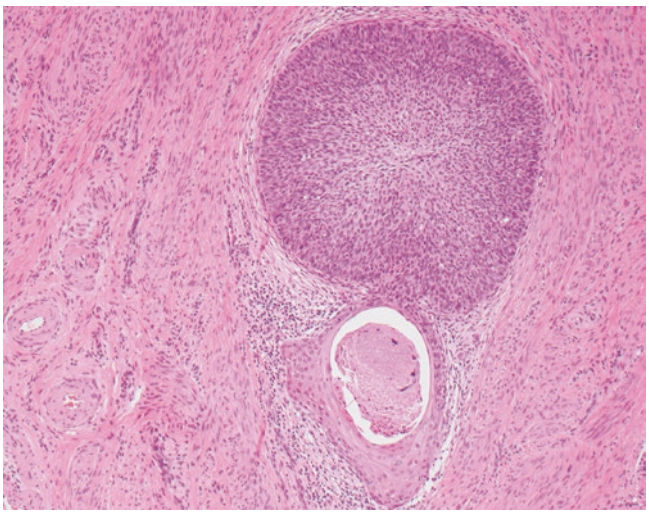

Fig. 7.39 Paradoxical maturation: Another example of paradoxical maturation with an invasive tongue of tumor emerging from a nest of high-grade squamous intraepithelial neoplasia

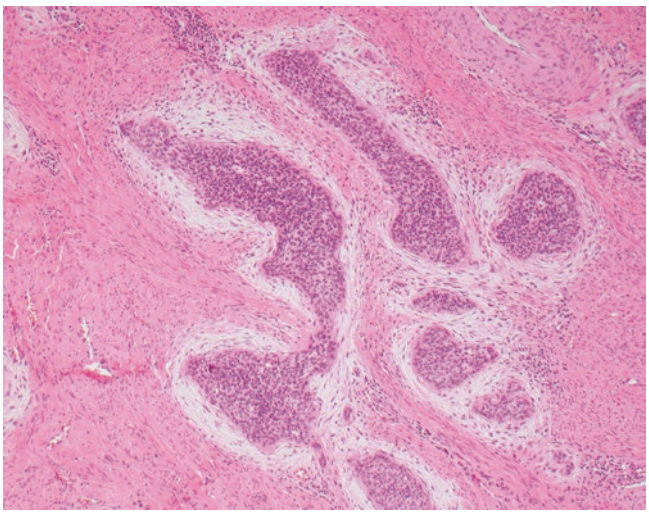

Fig. 7.41 Desmoplasia: A desmoplastic stromal reaction is a helpful indicator of invasion whenever it appears

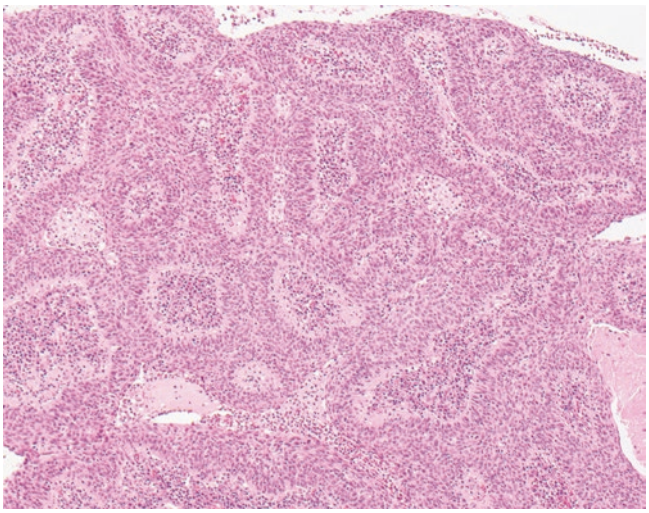

Fig. 7.40 Challenging invasion pattern: Confirming invasion may be more challenging in non-keratinizing and basaloid tumors, which lack paradoxical maturation and may not always provoke a prominent desmoplastic reaction. In such cases, the bulky distribution of tumor on a well-oriented section and the extension well beyond pre-existing endocervical glands confirms the presence of invasion

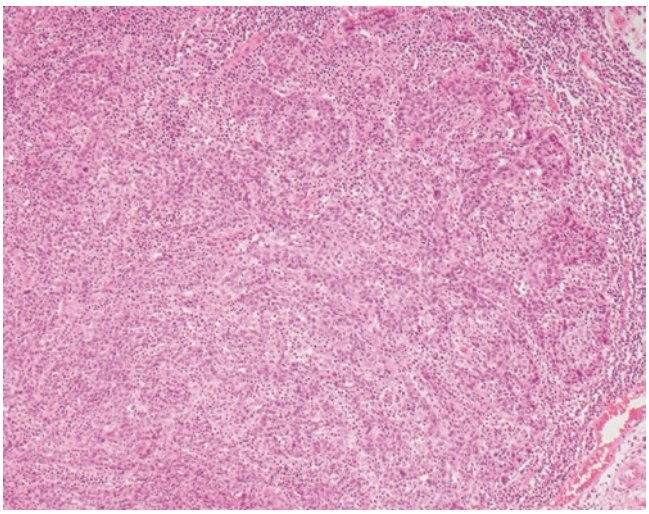

Fig. 7.42 Lymphoid infiltration: A robust associated lymphoid reaction can help secure the diagnosis of invasive squamous cell carcinoma when the epithelial component has an appropriately infiltrative pattern, but intraepithelial lesions also may have a dense inflammatory response

7.6.2 Patterns of Invasion

An awareness of different patterns of infiltration is also important when assessing the depth of invasion. The irregularly shaped invasive nests (jagged invasion) typical of many keratinizing squamous cell carcinomas are readily recognized as malignant owing to an overtly infiltrative appearance and prominent associated desmoplasia (Fig. 7.43). A spray-like pattern of invasion, characterized by tiny nests of hypermature squamous cells, is also easily classified as malignant (Fig. 7.44). Tongue-like invasion is also straightforward to diagnose: it consists of irregular protrusions of

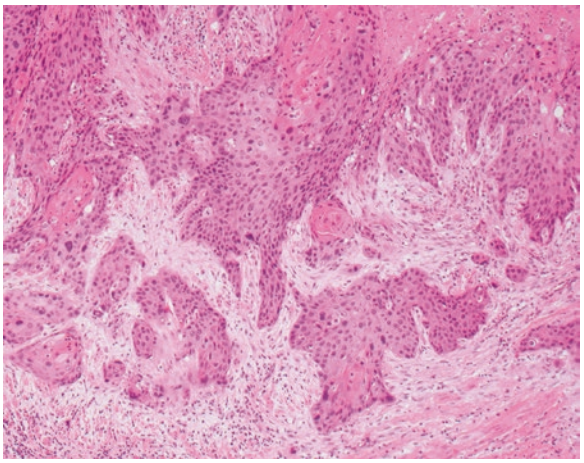

Fig. 7.43 Jagged invasion: Invasion is readily identified in cases that show a jagged infiltration pattern like the one depicted here

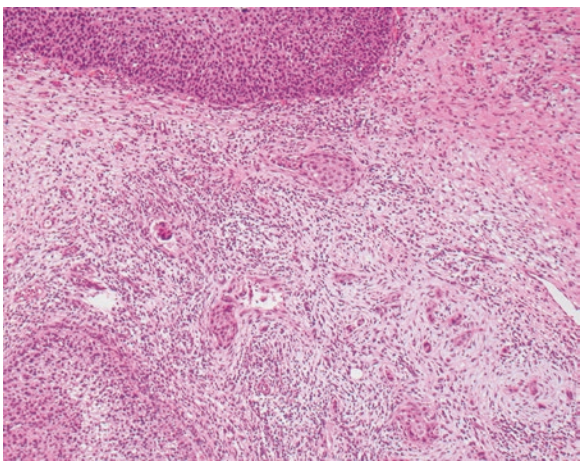

Fig. 7.44 "Spray pattern" of Invasion: Small, irregular clusters of tumor cells embedded in desmoplasia are typical of this pattern and represent one form of tumor budding

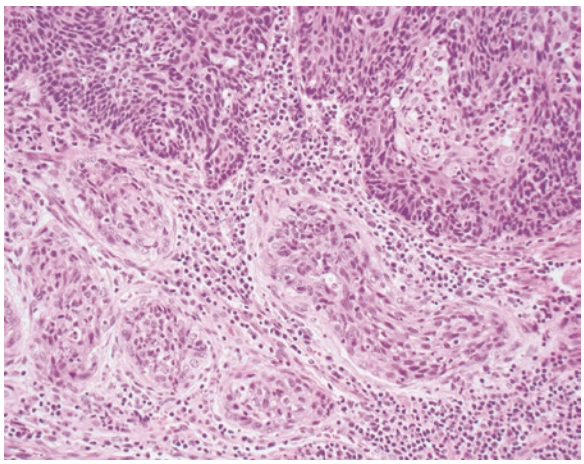

Fig. 7.45 Tongue-like invasion: Smooth tongues of tumor, another common pattern of invasion, are typically associated with a desmoplastic response. This case also shows a prominent lymphoid reaction

paradoxically mature cells, typically in association with a stromal reaction (Fig. 7.45).

Invasion is more challenging to diagnose when it manifests as confluent infiltration by a pushing border or more rounded nests of invasive tumor. This pattern of invasion can be difficult to differentiate from overlying intraepithelial lesions, particularly if the carcinoma has a basaloid or non-keratinizing morphology (Fig. 7.46). In such cases, paradoxical maturation is typically lacking, but a stromal reaction around the infiltrative nests and distribution beyond the expected pattern of endocervical glands help to secure the diagnosis of invasive malignancy.

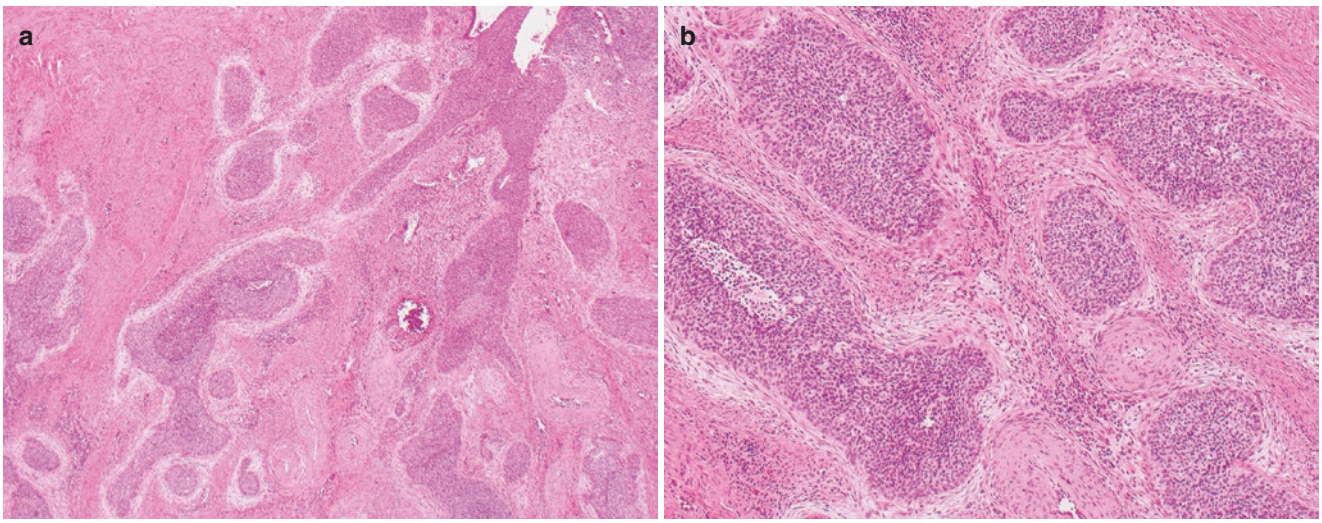

Fig. 7.46 Pushing invasion: This pattern can be challenging to differentiate from overlying HSIL, particularly when the tumor has basaloid morphology like the cancer illustrated here (**a** and **b**). The rind of reactive stroma is useful for confirming the presence of invasion, as is the extensive distribution of the neoplastic nests

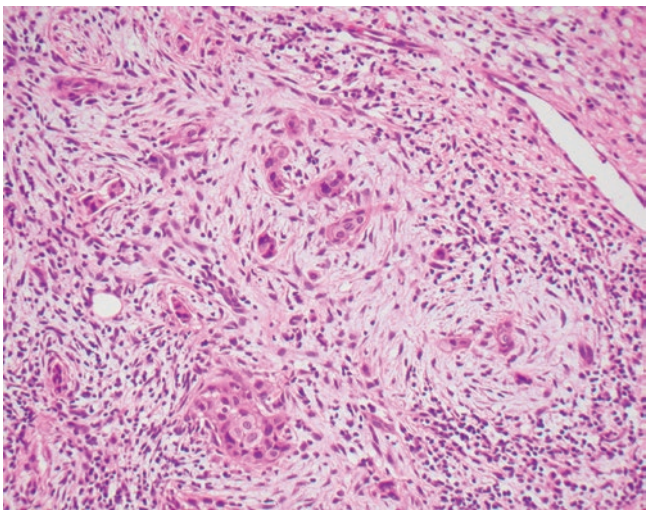

Fig. 7.47 Spray pattern of tumor budding: This higher-power view of the case pictured in Fig. 7.44 illustrates the minute nests of cells characteristic of this invasive pattern, which qualify as tumor budding and have been associated with worsened prognosis in some studies

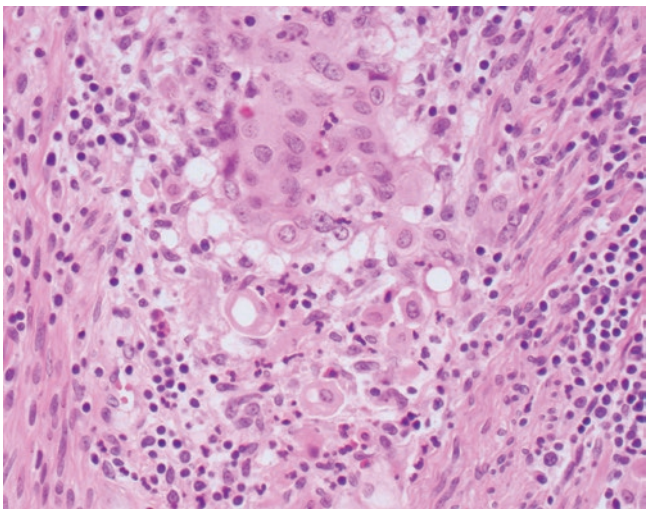

Fig. 7.48 Single-cell pattern of tumor budding: Tumor budding also may manifest as single cells "dripping" off a larger nest

The prognostic significance of these invasive patterns is not entirely clear. Some evidence suggests that certain patterns may be associated with worse outcome. Extrapolation from other organs indicates that the presence of tumor buds (including those seen in spray-like invasion) may have clinical significance; indeed, emerging data have suggested that high-level budding imparts a worsened prognosis in cervical squamous cell carcinoma [24–26, 53] (Figs. 7.47 and 7.48).

7.6.3 Depth of Invasion and Staging

Depth of invasion should be measured from the base of the epithelium to the point of maximum infiltration (Fig. 7.49). The non-invasive epithelium used to determine the baseline epithelial-stromal junction may be non-neoplastic or involved by intraepithelial neoplasia. There is an important caveat: if tumor arises from an endocervical gland populated by HSIL, the measurement should begin at the bottom of the involved gland, rather than at the epithelial-stromal junction.

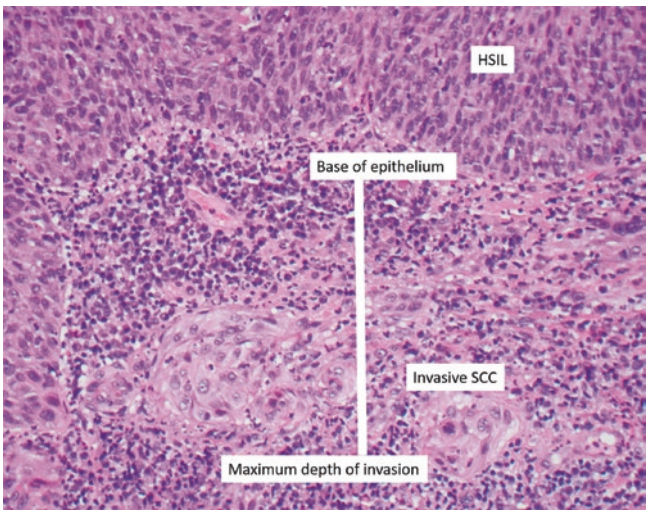

Fig. 7.49 Measuring depth of invasion: Depth of invasion should be measured from the baseline junction between the epithelium and the stroma to the point of deepest infiltration

Appropriately measuring invasion is critical for correct tumor staging, particularly for cases at the threshold of FIGO IA1 *versus* IA2, the point beyond which conservative management (such as complete conization) is no longer advisable. Stage IA1 is restricted to tumors with ≤3 mm of invasion. (Historically, horizontal extent ≤7 mm was also required, but it is not applicable in the most up-to-date FIGO system.) Historically, various terms have been enlisted for such cases, including "microinvasive carcinoma" and "early stromal invasion." The Lower Anogenital Squamous Terminology (LAST) Project, a working group that incorporated data derived from nearly 200 papers identified among 1863 candidate studies, recommends exclusive use of the term "superficially invasive squamous cell carcinoma" to avoid confusion, although the term "microinvasive" is still used with some frequency, particularly in the gynecologic oncology literature [48]. Nonetheless, many pathologists still avoid this terminology since measurement of depth of invasion takes precedence over descriptive terminology. Ascertaining the exact depth of invasion is also important for cases at the threshold of FIGO IA2 *versus* IB, as cases with >5 mm of invasion are classified as FIGO IB, with further subdivision based on the overall tumor dimension. Staging is discussed in further detail in Sect. 7.12.

7.6.4 Cervical Stromal Involvement by Thirds

Although none of the staging systems in current use assess depth of invasion as a function of overall cervical stromal thickness, many gynecologic oncology studies have found that involvement of the middle and/or outer third of the cervical stroma in hysterectomy specimens represents an adverse prognostic factor that may prompt escalated radiation therapy [54–57]. Thus, although this factor is not included in the current cervical carcinoma template of the College of American Pathologists (CAP), it is advisable to comment on whether the inner, middle, or outer third of the cervical stroma is involved when reporting cervical squamous cell carcinoma in a hysterectomy specimen.

Diagnostic Highlights

- Depth of invasion assessment is challenging due to tangential sectioning, involvement of endocervical glands by HSIL, and difficult patterns
- Involvement of endocervical glands by HSIL shows rounded contours, lack of prominent desmoplasia, and normal endocervical distribution
- Basaloid carcinomas often lack paradoxical maturation, increasing reliance on stromal reaction and distribution beyond normal endocervical glands
- Depth of invasion measured from epithelial junction except when invading from an endocervical gland populated by HSIL

7.6.5 Cases

1. A 32-year-old woman with bulky HSIL mimicking invasive squamous cell carcinoma (Fig. 7.36)
2. A 28-year-old woman with endocervical involvement by HSIL (Fig. 7.37)
3. A 35-year-old woman with squamous cell carcinoma demonstrating paradoxical maturation (Fig. 7.38)
4. A 35-year-old woman with squamous cell carcinoma demonstrating paradoxical maturation (Fig. 7.39)
5. A 38-year-old woman with basaloid squamous cell carcinoma with a challenging pattern of invasion (Fig. 7.40)
6. A 47-year-old woman with squamous cell carcinoma showing a strong desmoplastic response (Fig. 7.41)
7. A 52-year-old woman with squamous cell carcinoma with a strong lymphoid response (Fig. 7.42)
8. A 63-year-old woman with squamous cell carcinoma showing a jagged pattern of invasion (Fig. 7.43)
9. A 55-year-old woman with squamous cell carcinoma demonstrating a spray pattern of invasion with a desmoplastic response (Fig. 7.44)
10. A 41-year-old woman with squamous cell carcinoma with a tongue-like pattern of invasion (Fig. 7.45)
11. A 39-year-old woman with squamous cell carcinoma with a basaloid morphology and a pushing pattern of invasion (Fig. 7.46)

7.7 Measuring Tumor

7.7.1 Horizontal/Lateral Extent

The tumor staging systems encoded in the AJCC eighth edition [53] and the FIGO 2009 recommendations include a measurement of horizontal/lateral extent (i.e. width), with FIGO IA1 classification requiring a measurement ≤7 mm. If invasive tumor is present on a single slide, the horizontal extent is measured on that slide. If, instead, tumor is identified on consecutive slides, width is determined by comparing the measurement on a single slide to the measurement derived from adding up all involved consecutive sections (section thickness about 3 mm) and reporting the larger number. This method of tumor measurement is controversial, however, since adding horizontal extent 2-dimensionally on an "opened" specimen can overestimate tumor size of a 3-dimensional tumor. Invasive tumor on non-consecutive sections should be reported as individual foci. Importantly, horizontal extent is no longer a component of the FIGO 2018 system, and subsequent updates to the AJCC may exclude this measurement. It remains a point of controversy.

7.7.2 Tumor Diameter

Tumor diameter accounts for the maximum tumor dimension in any direction and is important for staging IB tumors. Historically, the important dividing line between IB1 and IB2 cases was at a threshold of ≤4 cm or >4 cm. The FIGO 2018 system has further subdivided IB to include a 2-cm cut-point, as tumors beneath this threshold appear to have lower rates of lymph node involvement and demonstrate improved overall outcome [58–61].

7.7.3 Multifocal Invasion

The LAST recommendations include multifocal invasive disease in the definition of stage T1A1 (FIGO IA1) superficially invasive squamous cell carcinoma. Multifocal invasion is defined as multiple invasive foci separated by a tissue block with no evidence of invasion in the intervening block(s), as invasive foci in the same block that are greater than 2 mm apart, or as invasive foci on different cervical lips (such as the anterior and posterior cervix) [53]. Reporting of multifocal, superficially invasive squamous cell carcinoma should include the number of foci, with overall stage based on the largest invasive focus [62].

Although there is no standard agreed-upon minimum intervening distance between multifocal invasive carcinoma, several authors arbitrarily have suggested 2 mm [62, 63]. A recent study that used the 2 mm interval distance found that 25% of FIGO 2009 stage IA1 invasive squamous cell carcinomas are multifocal [63]. In this study, patients with stage IA1 multifocal superficially invasive SCC had excellent prognosis, similar to that of patients with unifocal IA1 disease. This is important because these women are often young, and fertility-sparing local excision, rather than hysterectomy, can be performed with excellent outcomes. If the arbitrary 2 mm interval were to be increased and the separate foci measured as a continuous focus, many patients would have been upstaged to FIGO 2009 IB, resulting in a more radical procedure (trachelectomy or hysterectomy). The authors also emphasize the importance of obtaining levels when an invasive focus is identified in order to more accurately measure the size of the tumor; intervening levels may reveal continuous disease rather than separate foci, resulting in (appropriately) increased stage [63]. Again, this is perhaps less of a pressing issue for staging in the updated FIGO system.

7.8 Lymphovascular Invasion

Lymphovascular invasion is defined by single or individual groups of tumor cells in endothelium-lined spaces (Fig. 7.50). The presence of an appreciable endothelial lining is critical for confirming this finding, and cleft-like spaces without such a lining should be considered processing artifact rather than true lymphovascular invasion [64]. Assessment for lymphovascular invasion is best performed away from the invasive front of the tumor to avoid over-calling such artifacts (Fig. 7.51). CD31 and D2–40 immunohistochemistry can be useful ancillary tests for

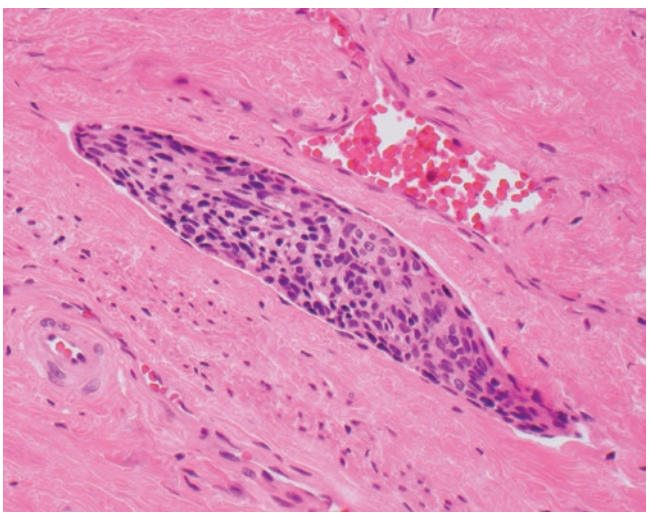

Fig. 7.50 Lymphovascular invasion: This involved lymphatic vessel shows a well-defined endothelium with tumor conforming to the vessel wall. The presence of an adjacent vascular channel is a helpful feature

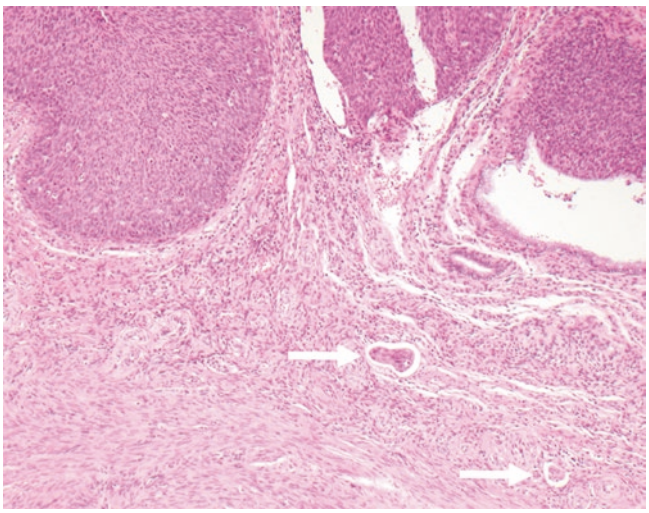

Fig. 7.51 Lymphovascular invasion: It is advisable to search for lymphovascular invasion away from the infiltrating front of the tumor, where retraction artifact may mimic lymphovascular involvement. These two involved vessels (*arrows*) are located distant from the rest of the invasive tumor (not pictured)

confirming venous and lymphatic invasion, respectively. There have been some attempts to differentiate between venous and lymphatic invasion, but the clinical significance of this distinction is thus far unclear [65].

The prognostic significance of lymphovascular invasion has not been robustly proven in squamous cervical carcinoma, and most studies have failed to show that it represents an independent risk factor for worsened outcome [66]; however, the presence of lymphovascular invasion has been shown to increase risk of nodal involvement [67]. Notably, the presence of lymphovascular invasion does not influence FIGO staging for superficially invasive cases, and, based on both the eighth edition of the AJCC Cancer Staging Manual [53] and the updated FIGO staging guidelines [68, 69], lymphovascular invasion may be identified in superficially invasive squamous cell carcinoma tumors without altering their IA1 stage. Furthermore, though some evidence has suggested that extensive lymphovascular invasion is associated with higher rates of nodal involvement in stage IB1 disease, this finding still does not directly impact staging [70].

That said, commentary on the presence or absence of lymphovascular invasion remains a critical component of pathologic assessment, as it may affect treatment approaches. Pelvic lymphadenectomy and modified radical hysterectomy warrant consideration in the context of lymphovascular involvement, even when invasion is limited and superficial [71, 72].

7.8.1 Cases

1. A 70-year-old woman with squamous cell carcinoma demonstrating lymphovascular invasion (Fig. 7.50)
2. A 51-year-old woman with squamous cell carcinoma demonstrating lymphovascular invasion (Fig. 7.51)

7.9 Perineural Invasion

Perineural invasion is defined by malignant cells immediately involving the perineural space of nerves; direct infiltration of the nerve itself is not necessary. This feature is of unclear prognostic significance in the cervix. Several studies have shown a decrease in recurrence-free and overall survival in the presence of this finding, but others have not [73–75]. Thus, while it is advisable to comment on the presence or absence of perineural invasion in pathology reports, it does not directly impact staging or management.

7.10 Extra-Cervical Involvement

7.10.1 Parametrial Involvement

Invasion into the parametrium is an important staging criterion for cervical squamous cell carcinomas; its involvement brings the FIGO stage to at least IIB [68]. The determination of involvement can be difficult, as the transition from endocervical tissue to parametrium is not well demarcated. Many consider invasion beyond the compact cervical stroma into the zone containing large caliber vessels or fat to be sufficient for classification as early invasion of the parametrium. Adequate sampling of the parametrial tissue remains necessary to ensure proper staging and margin status.

7.10.2 Involvement of Uterine Corpus and Adnexa

Involvement of the uterine corpus is disregarded in the current FIGO staging system, having no impact on stage; however, such involvement increases the risk of para-aortic lymph node and ovarian metastases [74]. Thus, there may be some clinical utility in including this information in the pathology report.

The 2018 update to the FIGO staging system specifically notes that ovarian involvement by squamous cell carcinoma is quite rare in early-stage cervical cancer (<1%), and the limited prognostic data on ovarian involvement preclude its inclusion in the staging criteria [68]. At least one study suggests that ovarian metastasis is a poor prognostic indicator, independent of histology, FIGO stage, or lymph node involvement [76], although others have not. The lack of inclusion of this and other adnexal involvement in cervical carcinoma staging remains controversial.

7.11 Lymph Node Involvement

Regional lymph nodes include pelvic nodes (parametrial, obturator, internal iliac [hypogastric], external iliac, common iliac, sacral, presacral) and para-aortic nodes. Pelvic lymphadenectomy is currently the surgical standard-of-care for cervical squamous cell carcinoma management, but recent studies have evaluated the potential of sentinel lymph node evaluation to reduce the morbidity of lymphadenectomy. In patients with early-stage cervical cancer, lymph node status is the most important prognostic factor [77]. Current guidelines recommend ultrastaging for sentinel lymph nodes to improve detection of metastases [53, 78]. There is no universal protocol for lymph node ultrastaging; individual institutions should have standard procedures for gross and microscopic evaluation of sentinel lymph nodes. For example, sentinel lymph nodes should be serially sectioned and submitted entirely for histologic evaluation. If no metastases are identified on H&E, levels and a cytokeratin-cocktail immunohistochemical stain should be performed on one or more sections [53, 78].

Minimal data are available to assign risk for non-sentinel lymph node metastasis based on the size of the metastasis in the sentinel lymph node; indeed, the current guidelines come from the breast carcinoma sizing of tumor deposits [53]. Micrometastases or macrometastatic involvement of any regional lymph nodes results in a TNM stage N1. The 2018 FIGO stage for pelvic lymph node involvement is IIIC1, and, for para-aortic involvement, it is IIIC2. Metastasis to lymph nodes outside of the regional nodal group is classified as distant metastasis (FIGO stage IVB) [53]. Micrometastases are defined as groups of tumor cells measuring >0.2 mm but not exceeding 2.0 mm. Any individual cluster of tumor cells exceeding 2.0 mm should be categorized as a macrometastasis. Separate micrometastatic foci—involving one or more nodes—should not be added together to determine the size of the metastasis; rather, a comment should describe how many micrometastatic deposits are identified. Isolated tumor cells (ITC) are single cells or small clusters of cells not exceeding 0.2 mm in greatest dimension, identified by histologic or immunohistochemical evaluation. Presence of isolated tumor cells in regional lymph node(s) should be staged as N0(i+) [53].

Although ultrastaging is recommended, identification of micrometastatic disease or isolated tumor cells in sentinel lymph nodes does not necessarily alter prognosis or treatment [79, 80]. The recent SENTICOL trial was the largest multi-institution clinical trial evaluating women with early-stage cervical carcinoma by sentinel lymph node mapping and subsequent ultrastaging. Ultrastaging did improve detection of lymph node micrometastases and ITCs, but the outcomes of patients with metastases at the time of surgery did not differ from those without metastases [79]. Additional trials with long-term follow-up are needed to further inform the prognosis of nodal isolated tumor cells or micrometastases.

Please also see Chap. 2 on specifics of lymph node processing, including sentinel lymph nodes, and measurement of tumor deposits.

7.12 Margin Status

The status of the surgical resection margins on hysterectomy (vaginal and parametrial) has a clear impact on overall survival, with statistically significant better outcomes for patients with negative margins. However, the effect of so-called "close margins" as a predictor of recurrence remains unclear. One study demonstrated a statistically significant difference: overall recurrence was 36% with 2-mm surgical margins *versus* 9% with 5-mm margins ($p = 0.009$) [81]. Another study showed similar local recurrence rates for negative margins (at least 1.0 cm) and close margins (10% *vs.* 11%), with significantly higher recurrence for positive margins (38%) [82]. Studying the effect of margins remains challenging because of the presence of other risk factors, and close margins may represent an intermediate risk for local recurrence [83].

7.13 Staging and Prognosis

Stage represents the most critical prognostic indicator for cervical squamous cell carcinoma, and it is the primary guide for treatment approach. The importance of stage is amplified by the fact that, unlike in many other malignancies, tumor histology and grade have little impact on the management of cervical squamous cancer. The most recent staging manual of the American Joint Committee on Cancer (AJCC) stages cervical carcinoma based on the 2009 recommendations of the International Federation of Gynecology and Obstetrics (FIGO). Both systems are codified in the College of American Pathologists (CAP) cervical carcinoma reporting template posted in August 2018 [53]. An update to the FIGO system was also released in 2018 but is not reflected in the AJCC eighth edition or in the subsequently released CAP cancer reporting template update [68, 69]. It should also be noted that there were several errors in the initial FIGO 2018 publication where the "=" was erroneously placed in 12 instances in Stages I and II. A corrigendum was subsequently published [84]. The staging systems currently in circulation therefore contain some discordances of which the pathologist should be aware (Table 7.2).

For instance, under the FIGO 2018 system, horizontal/lateral spread is no longer considered in sub-staging IA tumors because this measurement is subject to sectioning artifact and interobserver disagreement and does not appear to have reproducible independent prognostic significance [68, 69]. Thus, depth of invasion remains the sole stratifier within this group of microscopically appreciable tumors. Cases showing ≤3 mm of invasion (including all superficially invasive SCC 1A [SISCCA] and so-called "microinvasive" cases) qualify as FIGO IA1, and those showing >3 and ≤ 5 mm of invasion meet criteria for FIGO 1A2. This distinction is critical because conservative management with complete conization is an option for IA1 cases without lymphovascular invasion, whereas the risk of nodal involvement in the IA2 cancers is sufficient to prompt radical hysterectomy and pelvic nodal dissection in appropriate candidates [71, 72]. Radiation therapy also represents a treatment option for patients who are not ideal surgical candidates [83, 85–87]. Although lymphovascular invasion is not incorporated in any of the staging systems, its presence can prompt more aggressive management of IA1 tumors [71, 72].

FIGO IB cases, which include cervix-limited tumors with >5 mm of invasion, are further subdivided based on overall dimension. Of note, this category previously included all "clinically visible" lesions, however, in the current FIGO system these tumors still qualify as IA if invasion is ≤5 mm. The prior staging iterations divided IB lesions based only on whether they were at least 4 cm in size, but the latest FIGO system further divides lesions by size: ≤2 cm (IB1), >2 to ≤4 cm (IB2), and >4 cm (IB3). The recommended management for these cases includes radical hysterectomy/trachelectomy and pelvic lymphadenectomy, with radiation therapy also an option for small IB1 disease and for patients with contraindications to surgery [85–89].

The 2018 FIGO system also incorporates the presence of positive lymph nodes for stage III tumors with the generation of a new category, IIIC, for cases with either radiographic or pathologic confirmation of positive lymph nodes. There is no corresponding pT stage for this variable, as nodal status is incorporated separately in the pN stage under the AJCC eighth edition system, and the pelvic *versus* para-aortic location of the nodes is not considered. Unlike in prior iterations of the AJCC guidelines, however, the eighth edition uses the modifier "i+" to include isolated tumor cells under nodal staging. In contrast, isolated tumor cells are not mentioned in the FIGO schemas. Locally advanced cancers, including those with pelvic nodal disease, are typically managed with a combination of cisplatin-based chemotherapy and radiation, but the role of isolated tumor cells in dictating treatment remains unclear, as these cells do not clearly impact progression-free survival [79]. The significance of isolated tumor cells is discussed in greater detail in Sect. 7.1.

Lastly, both the 2009 and 2018 FIGO systems include distant metastases status under subdivisions of stage IV, whereas, in the AJCC system, this is addressed under the pM category. Cases with distant metastases are typically managed with cisplatin-based chemotherapy, with or without associated radiation [90]. Unfortunately, response rates remain low, with an average survival of 7 months. This has prompted consideration of additional treatment avenues, including the use of checkpoint inhibition in metastatic disease [91–94].

Table 7.2 A Comparison of AJCC eighth edition, FIGO 2009, and FIGO 2018 cervical carcinoma staging systems

Stage	AJCC eighth Edition	FIGO 2009	FIGO 2018
pT0	**No evidence of primary tumor**	**N/A**	**N/A**
pT1 (I)	**Confined to uterus**[a]	**Confined to uterus**[a]	**Confined to uterus**[a]
pT1a (IA)	Diagnosed only by microscopy, maximum depth ≤ 5 mm; horizontal spread ≤7 mm	Diagnosed only by microscopy, maximum depth ≤ 5 mm; horizontal spread ≤7 mm	Diagnosed only by microscopy, maximum depth ≤ 5 mm
pT1a1 (IA1)	*Invasion ≤ 3 mm; horizontal spread ≤ 7 mm*	*Invasion ≤ 3 mm; horizontal spread ≤ 7 mm*	*Invasion ≤ 3 mm*
pT1a2 (IA2)	*Invasion > 3 mm, ≤5 mm; horizontal spread ≤ 7 mm*	*Invasion > 3 mm, ≤5 mm; horizontal spread ≤ 7 mm*	*Invasion > 3 mm, ≤5 mm*
pT1b (IB)	Clinically visible lesion and/or microscopic lesion >T1a2	Clinically visible lesion and/or microscopic lesion >T1a2	Invasion >5 mm
pT1b1 (IB1)	*≤4 cm greatest dimension*	*≤4 cm greatest dimension*	*≤2 cm greatest dimension*
pT1b2 (IB2)	*>4 cm greatest dimension*	*>4 cm greatest dimension*	*>2 cm, ≤4 cm greatest dimension*
IB3	*N/A*	*N/A*	*>4 cm greatest dimension*
pT2 (II)	**Invades beyond uterus, but without involvement of the lower 1/3 of vagina or pelvic sidewall**	**Invades beyond uterus, but without involvement of the lower 1/3 of vagina or pelvic sidewall**	**Invades beyond uterus, but without involvement of the lower 1/3 of vagina or pelvic sidewall**

Table 7.2 (continued)

Stage	AJCC eighth Edition	FIGO 2009	FIGO 2018
pT2a (IIA)	Involvement of upper 2/3 of vagina without parametrial involvement	Involvement of upper 2/3 of vagina without parametrial involvement	Involvement of upper 2/3 of vagina without parametrial involvement
pT2a1 (IIA1)	*≤4 cm greatest dimension*	*≤4 cm greatest dimension*	*≤4 cm greatest dimension*
pT2a2 (IIA2)	*>4 cm greatest dimension*	*>4 cm greatest dimension*	*>4 cm greatest dimension*
pT2b (IIB)	With parametrial involvement	With parametrial involvement	With parametrial involvement
pT3 (III)	**Involves lower 1/3 of vagina and/or pelvic sidewall and/or causes hydronephrosis or nonfunctioning kidney**	**Involves lower 1/3 of vagina and/or pelvic sidewall[b] and/or causes hydronephrosis or nonfunctioning kidney.**	**Involves lower 1/3 of vagina and/or extends to pelvic sidewall and/or causes hydronephrosis or nonfunctioning kidney and/or involves pelvic/para-aortic lymph nodes**
pT3a (IIIA)	Involves lower 1/3 of vagina with no extension to pelvic sidewall	Involves lower 1/3 of vagina with no extension to pelvic sidewall	Involves lower 1/3 of vagina with no extension to pelvic sidewall
pT3b (IIIB)	Extends to pelvic sidewall and/or hydronephrosis or nonfunctioning kidney related to carcinoma	Extends to pelvic sidewall and/or hydronephrosis or nonfunctioning kidney related to carcinoma	Extends to pelvic sidewall and/or hydronephrosis or nonfunctioning kidney related to carcinoma
IIIC	N/A	N/A	Involvement of pelvic and/or para-aortic lymph nodes (including micrometastasis), irrespective of tumor size or extent (add *r* and *p* notations to specify radiologic *vs.* pathology confirmation)
IIIC1	*N/A*	*N/A*	*Pelvic lymph node metastases only*
IIIC2	*N/A*	*N/A*	*Para-aortic lymph node metastases*
pT4 (IV)	**Extends beyond the true pelvis and/or has involvement of bladder mucosa or rectum[c]**	**Extends beyond the true pelvis and/or has clinical involvement of bladder mucosa or rectum[c]**	**Extends beyond the true pelvis and/or has biopsy-proven involvement of bladder mucosa or rectum**
IVA	N/A	Spread to adjacent pelvic organs	Spread to adjacent pelvic organs
IVB	N/A	Spread to distant organs	Spread to distant organs
pN0	No regional lymph node metastases	N/A	N/A
pN0(i+)	Isolated tumor cells in regional lymph nodes ≤0.2 mm	N/A	N/A
pN1	Regional lymph node metastases	N/A	N/A
pM1	Distant metastases including peritoneal spread; involvement of supraclavicular, mediastinal, or distant lymph nodes; lung, liver, or bone involvement	N/A	N/A

AJCC American Joint Committee on Cancer, *FIGO* International Federation of Gynecology and Obstetrics
a: Uterine corpus involvement does not impact staging for any of the systems
b: Both FIGO systems clarify that pelvic sidewall involvement is defined as the absence of cancer-free space between tumor and pelvic sidewall. The pelvic sidewall includes the muscle, fascia, neurovascular structures, and skeletal portions of the bony pelvis
c: Bullous edema is not sufficient to classify as involvement under any of the three systems. The 2018 FIGO system specifies that biopsy-proven involvement is required

7.14 Predictive Biomarkers

The recent US Food and Drug Administration (FDA) approval of the anti-PD-1 checkpoint inhibitor pembrolizumab for the treatment of recurrent and advanced cervical squamous cell carcinoma has led to the use of PD-L1 immunohistochemistry as a predictive biomarker in this setting (Fig. 7.52) [94, 95]. Patient candidacy for this drug is based on a PD-L1 combined positive score (CPS) of at least 1. The CPS is based on the total number of PD-L1-positive tumor cells, macrophages, and lymphocytes divided by the total number of tumor cells present, multiplied by 100. Practically speaking, this means that more than 80% of cervical cancer patients will qualify, because only a single positive cell—be it tumor, macrophage, or lymphocyte—is required per 100 tumor cells in order to attain the minimum score of 1 [96].

Occasionally, immunohistochemical staining for DNA mismatch repair proteins is requested for cervical cancers, owing to the approval of pembrolizumab in all mismatch repair-deficient solid tumors [97, 98]. Given the rarity of mismatch repair deficiency in cervical squamous cell carcinoma and the high frequency of PD-L1 positivity of CPS ≥ 1 in these tumors, such testing is generally imprudent until PD-L1 immunohistochemistry is first performed, as patients are far more likely to qualify via that pathway.

Overall, checkpoint inhibitor-based immunotherapy has shown promise in a subset of patients with cervical squamous cell carcinoma, but it fails to provide a durable response for most [92, 93, 95]. Given that most cervical cancers enlist multiple mechanisms of immune evasion, combination approaches that target multiple immune modulatory molecules are of interest in cervical squamous carcinoma and may ultimately lead to an expansion of the predictive biomarkers enlisted clinically [99].

7.14.1 Case

A 45-year-old woman with squamous cell carcinoma demonstrating strong PD-L1 expression in tumor cells and the associated lymphoid infiltrate (Fig. 7.52).

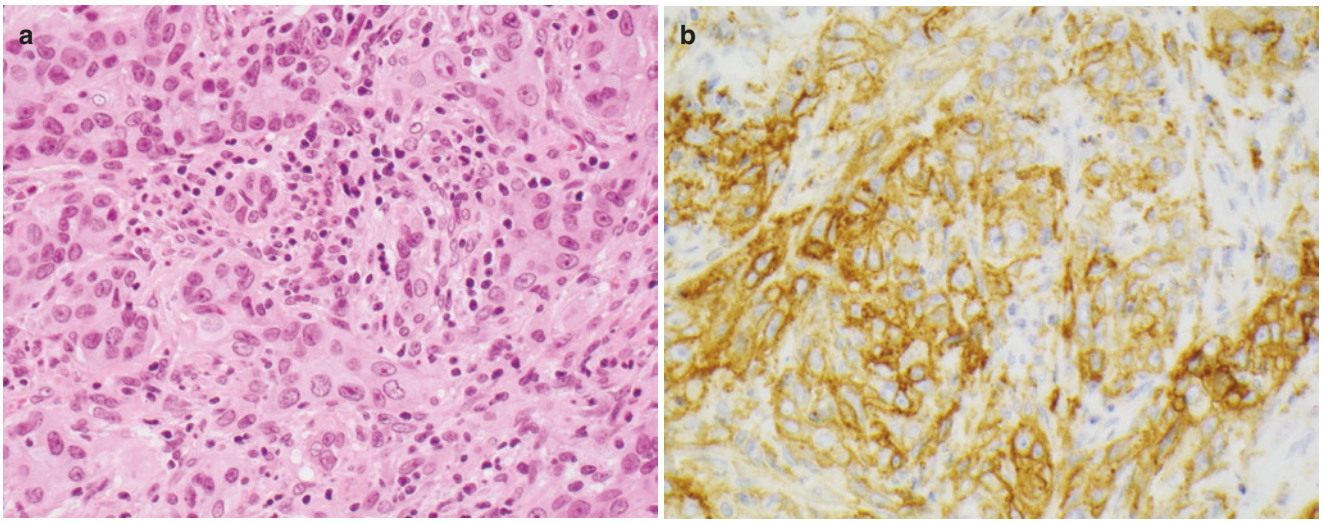

Fig. 7.52 PD-L1 immunohistochemistry in cervical squamous cell carcinoma: This squamous cell carcinoma (**a**) shows strong PD-L1 expression (**b**) not only in tumor cells, but also in associated inflammatory cells. This high level of positivity is well beyond the FDA-approved pembrolizumab treatment threshold of a combine positive score (CPS) ≥1

References

1. de Sanjose S, Quint WG, Alemany L, Geraets DT, Klaustermeier JE, Lloveras B, et al. Retrospective International Survey and HPV Time Trends Study Group. Human papillomavirus genotype attribution in invasive cervical cancer: a retrospective cross-sectional worldwide study. Lancet Oncol. 2010;11:1048–56.
2. Guimerà N, Lloveras B, Lindeman J, Alemany L, van de Sandt M, Alejo M, et al. The occasional role of low-risk human papillomaviruses 6, 11, 42, 44, and 70 in anogenital carcinoma defined by laser capture microdissection/PCR methodology: results from a global study. Am J Surg Pathol. 2013;37:1299–310.
3. Nicolás I, Marimon L, Barnadas E, Saco A, Rodríguez-Carunchio L, Fusté P, et al. HPV-negative tumors of the uterine cervix. Mod Pathol. 2019;32:1189–96.
4. Clifford GM, Smith JS, Plummer M, Muñoz N, Franceschi S. Human papillomavirus types in invasive cervical cancer worldwide: a meta-analysis. Br J Cancer. 2003;88:63–73.
5. Halec G, Alemany L, Lloveras B, Schmitt M, Alejo M, Bosch FX, et al. Retrospective International Survey and HPV Time Trends Study Group; Retrospective International Survey and HPV Time Trends Study Group. Pathogenic role of the eight probably/possibly carcinogenic HPV types 26, 53, 66, 67, 68, 70, 73 and 82 in cervical cancer. J Pathol. 2014;234:441–51.
6. Burk RD, Chen Z, Saller C, Tarvin K, Carvalho AL, Scapulatempo-Neto C, et al. Integrated genomic and molecular characterization of cervical cancer. Nature. 2017;543:378–84.
7. van Baars R, van der Marel J, Snijders PJ, Rodriquez-Manfredi A, ter Harmsel B, van den Munckhof HA, et al. CADM1 and MAL methylation status in cervical scrapes is representative of the most severe underlying lesion in women with multiple cervical biopsies. Int J Cancer. 2016;138:463–71.
8. Del Pino M, Sierra A, Marimon L, Martí Delgado C, Rodriguez-Trujillo A, Barnadas E, et al. CADM1, MAL, and miR124 promoter methylation as biomarkers of transforming cervical intrapithelial lesions. Int J Mol Sci. 2019;20:2262. https://doi.org/10.3390/ijms20092262.
9. Bray F, Ferlay J, Soerjomataram I, Siegel RL, Torre LA, Jemal A. Global cancer statistics 2018: GLOBOCAN estimates of incidence and mortality worldwide for 36 cancers in 185 countries. CA Cancer J Clin. 2018;68:394–424.
10. Grayson W, Cooper K. A reappraisal of "Basaloid carcinoma" of the cervix, and the differential diagnosis of basaloid cervical neoplasms. Adv Anat Pathol. 2002;9:290–300.
11. Koenig C, Turnicky RP, Kankam CF, Tavassoli FA. Papillary squamotransitional cell carcinoma of the cervix: a report of 32 cases. Am J Surg Pathol. 1997;21:915–21.
12. Albores-Saavedra J, Young RH. Transitional cell neoplasms (carcinomas and inverted papillomas) of the uterine cervix: a report of five cases. Am J Surg Pathol. 1995;19:1138–45.
13. Randall ME, Andersen WA, Mills SE, Kim JAC. Papillary squamous cell carcinoma of the uterine cervix: a clinicopathologic study of nine cases. Int J Gynecol Pathol. 1986;5:1–10.
14. Cho NH, Joo HJ, Ahn HJ, Jung WH, Lee KG. Detection of human papillomavirus in warty carcinoma of the uterine cervix: Comparison of immunohistochemistry, in situ hybridization and in situ polymerase chain reaction methods. Pathol Res Pract. 1998;194:713–20.
15. Parra-Herran C, Herfs M, Doria M, Crum CP, Nucci MR. Giant condyloma of the cervix: an uncommon entity associated with low-risk human papilloma virus infection. Am J Surg Pathol. 2013;37:300–4.
16. Robertson DI, Maung R, Duggan MA. Verrucous carcinoma of the genital tract: Is it a distinct entity? Can J Surg. 1993;36:147–51.
17. Bais AG, Kooi S, Teune TM, Ewing PC, Ansink AC. Lymphoepithelioma-like carcinoma of the uterine cervix: absence of Epstein-Barr virus, but presence of a multiple human papillomavirus infection. Gynecol Oncol. 2005;97:716–8.
18. Chao A, Tsai CN, Hsueh S, Lee LY, Chen TC, Huang SL, et al. Does Epstein-Barr virus play a role in lymphoepithelioma-like carcinoma of the uterine cervix? Int J Gynecol Pathol. 2009;28:279–85.
19. Eggen T, Arnes M, Moe B, Straume B, Ørbo A. Prognosis of early cervical cancer (FIGO stages IA2, IB, and IIA) in northern Norway predicted by malignancy grading score and objective morphometric image analysis. Int J Gynecol Pathol. 2007;26:447–56.
20. Bichel P, Jakobsen A. Histopathologic grading and prognosis of uterine cervical carcinoma. Am J Clin Oncol. 1985;8:247–54.
21. Graflund M, Sorbe B, Hussein A, Bryne M, Karlsson M. The prognostic value of histopathologic grading parameters and microvessel density in patients with early squamous cell carcinoma of the uterine cervix. Int J Gynecol Cancer. 2002;12:32–41.
22. Kristensen GB, Abeler VM, Risberg B, Tropé C, Bryne M. Tumor size, depth of invasion, and grading of the invasive tumor front are the main prognostic factors in early squamous cell cervical carcinoma. Gynecol Oncol. 1999;74:245–51.
23. Horn LC, Fischer U, Raptis G, Bilek K, Hentschel B, Richter CE, et al. Pattern of invasion is of prognostic value in surgically treated cervical cancer patients. Gynecol Oncol. 2006;103:906–11.
24. McCluggage WG. Towards developing a meaningful grading system for cervical squamous cell carcinoma. J Pathol Clin Res. 2018;4:81–5.
25. Jesinghaus M, Strehl J, Boxberg M, Brühl F, Wenzel A, Konukiewitz B, et al. Introducing a novel highly prognostic grading scheme based on tumour budding and cell nest size for squamous cell carcinoma of the uterine cervix. J Pathol Clin Res. 2018;4:93–102.
26. Huang B, Cai J, Xu X, Guo S, Wang Z. High-grade tumor budding stratifies early-stage cervical cancer with recurrence risk. PLoS One. 2016;11:e0166311. https://doi.org/10.1371/journal.pone.0166311.
27. Jenkins TM, Shojaei H, Song SJ, Schwartz LE. Role of Ancillary techniques in cervical biopsy and endocervical curettage specimens as follow-up to Papanicolaou test results indicating a diagnosis of atypical squamous cells, cannot exclude high-grade squamous intraepithelial lesion, or high-grade squamous intraepithelial lesion. Acta Cytol. 2020;64:155–65. https://doi.org/10.1159/000498888.
28. van Diepen DA, Hellebrekers B, van Haaften AM, Natté R. Cervical deciduosis imitating dysplasia. BMJ Case Rep 2015;2015. https://doi.org/10.1136/bcr-2015-210030.
29. Chapman GW, Savage EW, Salem FA. Cervical deciduosis and intraepithelial neoplasia. J Natl Med Assoc. 1979;71:787–9.
30. Kurman RJ, Carcangiu ML, Herrington CS, Young RH, editors. WHO classification of tumours of female reproductive organs, vol. 6. 4th ed. Lyon: IARC; 2014.
31. Shih IM, Kurman RJ. Epithelioid trophoblastic tumor: a neoplasm distinct from choriocarcinoma and placental site trophoblastic tumor simulating carcinoma. Am J Surg Pathol. 1998;22:1393–403.
32. Jordan S, Randall LM, Karamurzin Y, Ward P, Lin F, Brewster W, Monk BJ. Differentiating squamous cell carcinoma of the cervix and epithelioid trophoblastic tumor. Int J Gynecol Cancer. 2011;21:918–22.
33. Fadare O, Parkash V, Carcangiu ML, Hui P. Epithelioid trophoblastic tumor: clinicopathological features with an emphasis on uterine cervical involvement. Mod Pathol. 2006;19:75–82.
34. Mao TL, Seidman JD, Kurman RJ, Shih IM. Cyclin E and p16 immunoreactivity in epithelioid trophoblastic tumor – an aid in differential diagnosis. Am J Surg Pathol. 2006;30:1105–10.
35. Castle PE, Pierz A, Stoler MH. A systematic review and meta-analysis on the attribution of human papillomavirus (HPV) in neuroendocrine cancers of the cervix. Gynecol Oncol. 2018;148:422–9.

36. Tempfer CB, Tischoff I, Dogan A, Hilal Z, Schultheis B, Kern P, Rezniczek GA. Neuroendocrine carcinoma of the cervix: a systematic review of the literature. BMC Cancer. 2018;18:530.
37. Burk RD, Terai M, Gravitt PE, Brinton LA, Kurman RJ, Barnes WA, et al. Distribution of human papillomavirus types 16 and 18 variants in squamous cell carcinomas and adenocarcinomas of the cervix. Cancer Res. 2003;63:7215–20.
38. Quddus MR, Manna P, Sung CJ, Kerley S, Steinhoff MM, Lawrence WD. Prevalence, distribution, and viral burden of all 15 high-risk human papillomavirus types in adenosquamous carcinoma of the uterine cervix: a multiplex real-time polymerase chain reaction-based study. Hum Pathol. 2014;45:303–9.
39. Lee H, Lee H, Cho YK. Cytokeratin7 and cytokeratin19 expression in high grade cervical intraepithelial neoplasm and squamous cell carcinoma and their possible association in cervical carcinogenesis. Diagn Pathol. 2017;12:18. https://doi.org/10.1186/s13000-017-0609-4.
40. Jung YY, Nahm JH, Kim HS. Cytomorphological characteristics of glassy cell carcinoma of the uterine cervix: histopathological correlation and human papillomavirus genotyping. Oncotarget. 2016;7:74152–61.
41. Koh SS, Cassarino DS. Immunohistochemical expression of p16 in melanocytic lesions: an updated review and meta-analysis. Arch Pathol Lab Med. 2018;142:815–28.
42. Alexander RE, Hu Y, Kum JB, Montironi R, Lopez-Beltran A, Maclennan GT, et al. p16 expression is not associated with human papillomavirus in urinary bladder squamous cell carcinoma. Mod Pathol. 2012;25:1526–33.
43. Rambau PF, Vierkant RA, Intermaggio MP, Kelemen LE, Goodman MT, Herpel E, et al. Association of p16 expression with prognosis varies across ovarian carcinoma histotypes: an Ovarian Tumor Tissue Analysis Consortium study. J Pathol Clin Res. 2018;4:250–61.
44. Yemelyanova A, Ji H, Shih I, Wang TL, Wu LS, Ronnett BM. Utility of p16 expression for distinction of uterine serous carcinomas from endometrial endometrioid and endocervical adenocarcinomas: immunohistochemical analysis of 201 cases. Am J Surg Pathol. 2009;33:1504–14.
45. El-Bahrawy M. Expression of p16 in post-radiotherapy cervical biopsies. Histopathology. 2011;58:1174–6.
46. Munger K, Gwin TK, McLaughlin-Drubin M. p16 in HPV-associated cancers. Oncotarget. 2013;4:1864–5.
47. Klaes R, Benner A, Friedrich T, Ridder R, Herrington S, Jenkins D, et al. p16INK4a immunohistochemistry improves interobserver agreement in the diagnosis of cervical intraepithelial neoplasia. Am J Surg Pathol. 2002;26:1389–99.
48. Darragh TM, Colgan TJ, Thomas Cox J, Heller DS, Henry MR, Luff RD, et al. The Lower Anogenital Squamous Terminology Standardization Project for HPV-associated lesions: background and consensus recommendations from the College of American Pathologists and the American Society for Colposcopy and Cervical Pathology. Int J Gynecol Pathol. 2013;32:76–115.
49. Rodríguez-Carunchio L, Soveral I, Steenbergen RDM, Torné A, Martinez S, Fusté P, et al. HPV-negative carcinoma of the uterine cervix: a distinct type of cervical cancer with poor prognosis. BJOG. 2015;122:119–27.
50. Pirog EC. Cervical adenocarcinoma: diagnosis of human papillomavirus-positive and human papillomavirus-negative tumors. Arch Pathol Lab Med. 2017;141:1653–67.
51. Mills AM, Dirks DC, Poulter MD, Mills SE, Stoler MH. HR-HPV E6/E7 mRNA in situ hybridization: Validation against PCR, DNA in situ hybridization, and p16 immunohistochemistry in 102 samples of cervical, vulvar, anal, and head and neck neoplasia. Am J Surg Pathol. 2017;41:607–15.
52. Rooper LM, Gandhi M, Bishop JA, Westra WH. RNA in-situ hybridization is a practical and effective method for determining HPV status of oropharyngeal squamous cell carcinoma including discordant cases that are p16 positive by immunohistochemistry but HPV negative by DNA in-situ hybridization. Oral Oncol. 2016;55:11–6.
53. Amin MB, Edge S, Greene F, Byrd DR, Brookland RK, Washington MK, et al., editors. AJCC cancer staging manual. 8th ed. New York: Springer; 2017.
54. Van De Putte G, Lie AK, Vach W, Baekelandt M, Kristensen GB. Risk grouping in stage IB squamous cell cervical carcinoma. Gynecol Oncol. 2005;99:106–12.
55. Delgado G, Bundy BN, Fowler WC, Stehman FB, Sevin B, Creasman WT, et al. A prospective surgical pathological study of stage I squamous carcinoma of the cervix: a Gynecologic Oncology Group study. Gynecol Oncol. 1989;35:314–20.
56. Ryu SY, Kim MH, Nam BH, Lee TS, Song ES, Park CY, et al. Intermediate-risk grouping of cervical cancer patients treated with radical hysterectomy: a Korean Gynecologic Oncology Group study. Br J Cancer. 2014;110:278–85.
57. Samlal RA, van der Velden J, Ten Kate FJ, Schilthuis MS, Hart AA, Lammes FB. Surgical pathologic factors that predict recurrence in stage IB and IIA cervical carcinoma patients with negative pelvic lymph nodes. Cancer. 1997;80:1234–40.
58. Kodama J, Fukushima C, Kusumoto T, Nakamura K, Seki N, Hongo A, Hiramatsu Y. Stage IB1 cervical cancer patients with an MRI-measured tumor size < or = 2 cm might be candidates for less-radical surgery. Eur J Gynaecol Oncol. 2013;34:39–41.
59. Kodama J, Mizutani Y, Hongo A, Yoshinouchi M, Kudo T, Okuda H. Optimal surgery and diagnostic approach of stage IA2 squamous cell carcinoma of the cervix. Eur J Obstet Gynecol Reprod Biol. 2002;101:192–5.
60. Horn L-C, Bilek K, Fischer U, Einenkel J, Hentschel B. A cut-off value of 2 cm in tumor size is of prognostic value in surgically treated FIGO stage IB cervical cancer. Gynecol Oncol. 2014;134:42–6.
61. Wagner AE, Pappas L, Ghia AJ, Gaffney DK. Impact of tumor size on survival in cancer of the cervix and validation of stage IIA1 and IIA2 subdivisions. Gynecol Oncol. 2013;129:517–21.
62. Day E, Duffy S, Bryson G, Syed S, Shanbhag S, Burton K, et al. Multifocal FIGO stage IA1 squamous carcinoma of the cervix: criteria for Identification, staging, and its good clinical outcome. Int J Gynecol Pathol. 2016;35:467–74.
63. McIlwaine P, Nagar H, McCluggage WG. Multifocal FIGO stage 1a1 cervical squamous carcinomas have an extremely good prognosis equivalent to unifocal lesions. Int J Gynecol Pathol. 2014;33:213–7.
64. Wittekind C, Brierley JD, Lee A, van Eycken E, editors. TNM supplement: a commentary on uniform use. 5th ed. Hoboken, NJ: Wiley-Blackwell; 2019.
65. Sakuragi N, Takeda N, Hareyama H, Fujimoto T, Todo Y, Okamoto K, et al. A multivariate analysis of blood vessel and lymph vessel invasion as predictors of ovarian and lymph node metastases in patients with cervical carcinoma. Cancer. 2000;88:2578–83.
66. Creasman WT, Morrow CP, Bundy BN, Homesley HD, Graham JE, Heller PB. Surgical pathologic spread patterns of endometrial cancer. A Gynecologic Oncology Group Study. Cancer. 1987;60:2035–41.
67. Pallavi VR, Devi KU, Mukherjee G, Ramesh C, Bafna UD. Relationship between lymph node metastases and histopathological parameters in carcinoma cervix: a multivariate analysis. J Obstet Gynaecol. 2012 Jan;32(1):78–80.
68. Bhatla N, Berek JS, Cuello Fredes M, Denny LA, Grenman S, Karunaratne K, et al. Revised FIGO staging for carcinoma of the cervix uteri. Int J Gynecol Obstet. 2019;145:129–35.
69. Bhatla N, Aoki D, Sharma DN, Sankaranarayanan R. Cancer of the cervix uteri. Int J Gynecol Obstet. 2018;143:22–36.
70. Chandacham A, Charoenkwan K, Siriaunkgul S, Srisomboon J, Suprasert P, Phongnarisorn C, et al. Extent of lymphovascular space invasion and risk of pelvic lymph node metastases in

stage IB1 cervical cancer. J Med Assoc Thail. 2005;88(Suppl 2):S31–6.
71. Sevin B-U, Nadji M, Averette HE, Hilsenbeck S, Smith D, Lampe B. Microinvasive carcinoma of the cervix. Cancer. 1992;70:2121–8.
72. Elliott P, Coppleson M, Russell P, Liouros P, Carter J, MacLeod C, Jones M. Early invasive (FIGO stage IA) carcinoma of the cervix: a clinico-pathologic study of 476 cases. Int J Gynecol Cancer. 2000;10:42–52.
73. Cui L, Shi Y, Zhang GN. Perineural invasion as a prognostic factor for cervical cancer: a systematic review and meta-analysis. Arch Gynecol Obstet. 2015;292:13–9.
74. Cho HC, Kim H, Cho HY, Kim K, No JH, Kim YB. Prognostic significance of perineural invasion in cervical cancer. Int J Gynecol Pathol. 2013;32:228–33.
75. Horn L-C, Meinel A, Fischer U, Bilek K, Hentschel B. Perineural invasion in carcinoma of the cervix uteri – prognostic impact. J Cancer Res Clin Oncol. 2010;136:1557–62.
76. Shimada M, Kigawa J, Nishimura R, Yamaguchi S, Kuzuya K, Nakanishi T, et al. Ovarian metastasis in carcinoma of the uterine cervix. Gynecol Oncol. 2006;101:234–7.
77. Holman LL, Levenback CF, Frumovitz M. Sentinel lymph node evaluation in women with cervical cancer. J Minim Invasive Gynecol. 2014;21:540–5.
78. Diaz JP, Gemignani ML, Pandit-Taskar N, Park KJ, Murray MP, Chi DS, et al. Sentinel lymph node biopsy in the management of early-stage cervical carcinoma. Gynecol Oncol. 2011;120:347–52.
79. Guani B, Dorez M, Magaud L, Buenerd A, Lecuru F, Mathevet P. Impact of micrometastasis or isolated tumor cells on recurrence and survival in patients with early cervical cancer: SENTICOL Trial. Int J Gynecol Cancer. 2019;29:447–52.
80. Delomenie M, Bonsang-Kitzis H, Bats AS, Ngo C, Balaya V, Xuan HTN, et al. The clinical implication of lymph nodes micrometastases and isolated tumor cells in patients with cervical cancer: a systematic review. Eur J Obstet Gynecol Reprod Biol. 2019;241:71–6.
81. McCann GA, Taege SK, Boutsicaris CE, Phillips GS, Eisenhauer EL, Fowler JM, et al. The impact of close surgical margins after radical hysterectomy for early-stage cervical cancer. Gynecol Oncol. 2013;128:44–8.
82. Viswanathan AN, Lee H, Hanson E, Berkowitz RS, Crum CP. Influence of margin status and radiation on recurrence after radical hysterectomy in stage IB cervical cancer. Int J Radiat Oncol Biol Phys. 2006;65:1501–7.
83. Khanna N, Rauh LA, Lachiewicz MP, Horowitz IR. Margins for cervical and vulvar cancer. J Surg Oncol. 2016;113:304–9.
84. Corrigendum to "Revised FIGO staging for carcinoma of the cervix uteri" [Int J Gynecol Obstet 145(2019) 129–135]. Int J Gynaecol Obstet. 2019;147(2):279–80.
85. Landoni F, Maneo A, Cormio G, Perego P, Milani R, Caruso O, Mangioni C. Class II versus class III radical hysterectomy in stage IB-IIA cervical cancer: a prospective randomized study. Gynecol Oncol. 2001;80:3–12.
86. Landoni F, Colombo A, Milani R, Placa F, Zanagnolo V, Mangioni C. Randomized study between radical surgery and radiotherapy for the treatment of stage IB–IIA cervical cancer: 20-year update. J Gynecol Oncol. 2017;28:e34.
87. Landoni F, Maneo A, Colombo A, Placa F, Milani R, Perego P, et al. Randomised study of radical surgery versus radiotherapy for stage Ib-IIa cervical cancer. Lancet. 1997;350:535–40.
88. Grigsby PW, Perez CA. Radiotherapy alone for medically inoperable carcinoma of the cervix: stage IA and carcinoma in situ. Int J Radiat Oncol Biol Phys. 1991;21:375–8.
89. Eifel PJ, Morris M, Wharton JT, Oswald MJ. The influence of tumor size and morphology on the outcome of patients with FIGO stage IB squamous cell carcinoma of the uterine cervix. Int J Radiat Oncol Biol Phys. 1994;29:9–16.
90. Moore DH, Blessing JA, McQuellon RP, Thaler HT, Cella D, Benda J, et al. Phase III study of cisplatin with or without paclitaxel in stage IVB, recurrent, or persistent squamous cell carcinoma of the cervix: A Gynecologic Oncology Group study. J Clin Oncol. 2004;22:3113–9.
91. Frenel JS, Le Tourneau C, O'Neil BH, Ott PA, Piha-Paul SA, Gomez-Roca CA, et al. Pembrolizumab in patients with advanced cervical squamous cell cancer: Preliminary results from the phase Ib KEYNOTE-028 study. J Clin Oncol. 2016;34(suppl):5515. https://doi.org/10.1200/JCO.2016.34.15_suppl.5515.
92. Frenel JS, Le Tourneau C, O'Neil B, Ott PA, Piha-Paul SA, Gomez-Roca CA, et al. Safety and efficacy of pembrolizumab in advanced, programmed death ligand 1-positive cervical cancer: results from the phase Ib KEYNOTE-028 Trial. J Clin Oncol. 2017;35:4035–41.
93. Borcoman E, Le Tourneau C. Pembrolizumab in cervical cancer: latest evidence and clinical usefulness. Ther Adv Med Oncol. 2017;9:431–9.
94. US Food and Drug Administration. FDA approves pembrolizumab for advanced cervical cancer with disease progression during or after chemotherapy. 2018. https://www.fda.gov/Drugs/InformationOnDrugs/ApprovedDrugs/ucm610572.htm.
95. Chung HC, Ros W, Delord JP, Perets R, Italiano A, Shapira-Frommer R, et al. Efficacy and safety of pembrolizumab in previously treated advanced cervical cancer: results from the phase II KEYNOTE-158 study. J Clin Oncol. 2019;37:1470–8.
96. Kulangara K, Hanks DA, Waldroup S, Peltz L, Shah S, Roach C, et al. Development of the combined positive score (CPS) for the evaluation of PD-L1 in solid tumors with the immunohistochemistry assay PD-L1 IHC 22C3 pharmDx. J Clin Oncol. 2017;35:e14589.
97. Marcus L, Lemery SJ, Keegan P, Pazdur R. FDA approval summary: pembrolizumab for the treatment of microsatellite instability-high solid tumors. Clin Cancer Res. 2019;25:3753–8.
98. Le DT, Durham JN, Smith KN, Wang H, Bartlett BR, Aulakh LK, et al. Mismatch-repair deficiency predicts response of solid tumors to PD-1 blockade. Science. 2017;357:409–13.
99. Chinn Z, Stoler MH, Mills AM. PD-L1 and IDO expression in cervical and vulvar invasive and intraepithelial squamous neoplasias: implications for combination immunotherapy. Histopathology. 2019;74:256–68.